

N7620176



NASA CR - 137812

NASA CONTRACTOR
REPORT

EXPERIMENTAL EVALUATION OF
OUTER PLANETS PROBE
THERMAL INSULATION CONCEPTS

By M. G. GROTE AND S. A. MEZINES

Prepared by

MCDONNELL DOUGLAS ASTRONAUTICS COMPANY — EAST
St. Louis, Missouri 63166 (314) 232-0232

NATIONAL AERONAUTICS AND SPACE ADMINISTRATION • WASHINGTON, D.C. • MARCH 1976

TABLE OF CONTENTS

	PAGE
TITLE PAGE	i
TABLE OF CONTENTS	ii
LIST OF FIGURES	iii
SYMBOLS	iv
ABSTRACT	vi
1. INTRODUCTION	1
2. HEAT TRANSFER IN A POROUS MEDIA	3
Effective Gas Conductivity	4
Gas Solid Thermal Conductivity	7
Solid Contact Conductivity	7
Radiation	7
Convection	8
Heat Transfer Model in a Porous Media	8
3. HEAT TRANSFER IN A HONEYCOMB CORE	9
4. SPECIMEN FABRICATION	12
5. TEST DEFINITION	16
6. TEST SETUP	18
7. TEST RESULTS	23
8. BOND STRENGTH TEST	29
9. DISCUSSION OF TEST DATA	31
10. ADDITIONAL TESTING	37
11. DISCUSSION OF THE RESULTS OF ADDITIONAL TESTING	39
12. CONCLUSIONS AND RECOMMENDATIONS	40
REFERENCES	41
ACKNOWLEDGEMENTS	42
APPENDICES	
A. PROPERTIES OF THE GASES AND FILLERS	43
B. THERMAL CONDUCTIVITY TEST APPARATUS	46
C. SOUTHERN RESEARCH INSTITUTE REPORT	48

LIST OF PAGES

Title Page
ii-through vi
1-64

LIST OF FIGURES

FIGURE	TITLE	PAGE
1	Outer Planet Probe	1
2	Typical Effective Thermal Conductivity of Porous Media	3
3	Parallel Heat Transfer Model	3
4	Mean Free Path of Helium Gas	5
5	Mean Pore Diameter for a 50-50 Mixture of Carbon Black & Cab-O-Sil	6
6	Rayleigh Number for Various Gases	10
7	Onset of Natural Convection in a Honeycomb Core Heated from Below	11
8	Nu for a Fiberglass Honeycomb Core Heated from Below	11
9	Specimen Configuration	13
10	Unassembled Test Specimen	13
11	Specimens Fabricated	14
12	V-Blender	14
13	Setup for Packing the Powder	15
14	Test Matrix	17
15	Test Setup Schematic	18
16	Thermal Conductivity Test Stack with Unheated Coldplates	19
17	Assembled Test Stack	20
18	Two Guarded Hotplate Calorimeter Setups Installed in a Vacuum Bell Jar	21
19	Two Guarded Hotplate Calorimeter Setups Installed in a High Pressure Autoclave	22
20	Test Data	24
21	H/C Core Material Conductivity	25
22	Thermal Conductivity Test Results	26
23	Specimen Thermal Conductivity in a Nitrogen Atmosphere	27
24	Specimen Thermal Conductivity in a Helium Atmosphere	28
25	Flatwise Tension Test Specimen	29
26	Flatwise Tension Test Setup	29
27	Flatwise Tension Test Data	30
28	Forward Honeycomb Core Flatwise Tension Test Results	30
29	Radial Temperature Distribution	31
30	Thermal Conductivity in a Helium Environment at One Atmosphere Pressure	32
31	Comparison of Experimental Results for Thermal Conductivity of MS-7 Powder Mixture in a Helium Environment	33
32	Comparison of Experimental Data to Analytic Value of k_{ge} at 300°K	34
33	Limiting Cases of Heat Transfer	35
34	ULD Conductivity at One Atmosphere Pressure	36
35	Redesigned Specimen Configuration	37
36	Redesigned Specimen Test Data	38

NOMENCLATURE

Å	Angstrom unit, 10^{-8} cm
A	Surface area of faceplate
A_s	Surface area of powder
C	Numerical constant
C_p	Specific heat at constant pressure
C_v	Specific heat at constant volume
D	Diameter of the honeycomb cell
Da	Darcy number = K/D^2
D_p	Diameter of powder particle
d	Diameter of gas molecule
f	Solid volume fraction of the filler, $\rho_{\text{Packed}}/\rho_{\text{solid material}}$
F	Solid volume fraction of the honeycomb core
g	Acceleration of gravity
h_r	Radiation heat transfer coefficient
i	Temperature discontinuity coefficient
K	Permeability of the porous media
k	Overall thermal conductivity of the specimen
k_{as}	Solid contact thermal conductivity
k_{conv}	Thermal conductivity due to convection
k_{Filler}	Thermal conductivity of the filler material
k_{ge}	Effective gas thermal conductivity in the porous media
k_{go}	Thermal conductivity of the unconfined gas
k_{gs}	Gas-solid thermal conductivity
$k_{H/C}$	Thermal conductivity of the honeycomb core
k_{rad}	Thermal conductivity due to radiation
k_s	Thermal conductivity of solid powder material
L	Height of the honeycomb core
L_e	Effective mean free path
L_g	Mean free path of the gas
L_p	Mean pore diameter of the filler
N	Avogadro's number - 6.023×10^{23} molecules/gm-mole
N_{bs}	Backscattering cross section
Nu	Nusselt number - k/k_{go}
n	Number of molecules per unit volume
P	Pressure-atmospheres
Q	Total heat

R	Universal gas constant
Ra	Rayleigh number, $\beta g \Delta T L^3 / \nu \kappa$
Ra _c	Critical Rayleigh number for the onset of natural convection
T	Temperature, °K
T _m	Mean specimen temperature
ΔT	Temperature difference between the upper and lower surfaces
V _a	Average molecular velocity
Y _p	Particle to particle conductance
α	Accommodation coefficient
β	Volume coefficient of expansion
γ	Ratio of specific heats, C _p /C _v
ρ	Density
σ	Stefan-Boltzman Constant, 5.67 x 10 ⁻⁸ watts/meter ² K ⁴
ν	Kinematic viscosity
ε	Surface emissivity
μ	Micron - 10 ⁻⁴ cm
κ	Thermal diffusivity, k _{go} /ρC _p

ABSTRACT

An experimental program was conducted to evaluate various thermal insulation concepts for use in the Outer Planets Probe (OPP) during entry and descent into the atmospheres of Jupiter, Saturn and Uranus. Phenolic fiberglass honeycomb specimens representative of the OPP structure were packed and tested with the following fillers:

- Unfilled
- 50-50 mixture carbon black/silica powder (CAB-O-SIL EH-5) filler
- 50-50 mixture carbon black/silica powder (CAB-O-SIL MS-7) filler
- Ultra low density (ULD) silicone elastomeric foam filler

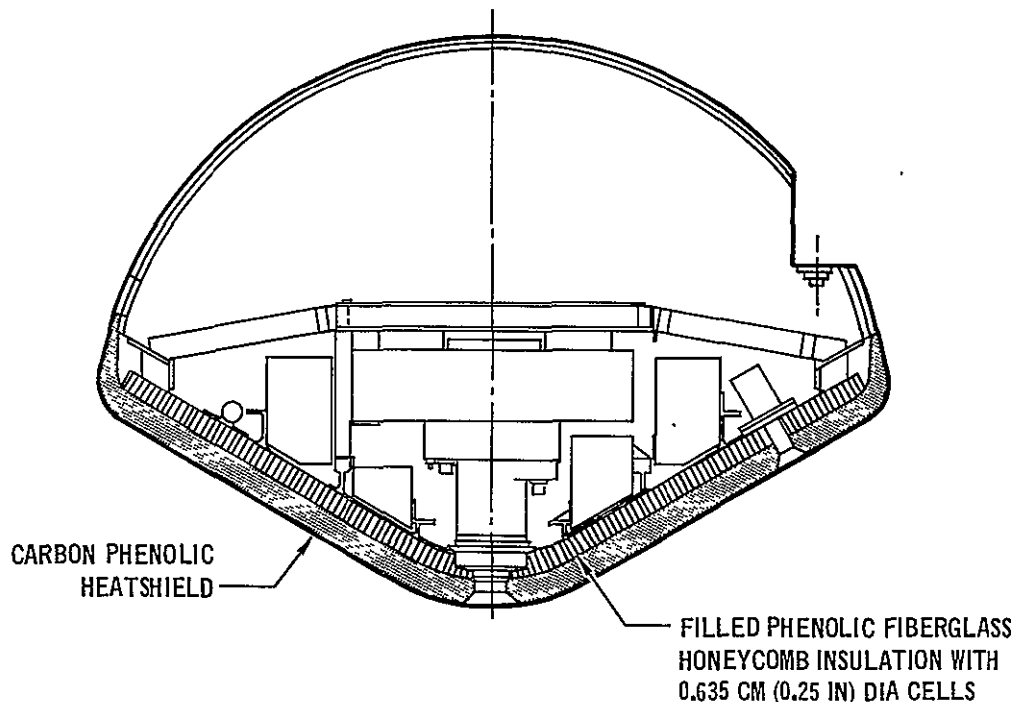
Thermal conductivity measurements were made at McDonnell Douglas Astronautics Company-East (MDAC-E) over a temperature range of 300°K to 483°K and pressures from vacuum up to 10 atmospheres in helium and nitrogen gas environments. The conductivity results could not be fully explained so new test specimens were designed with improved venting characteristics, and tested at an independent research laboratory to determine the validity of the original data. All of the conductivity data showed results that were substantially higher than expected. The original test data in helium were lower than the data from the redesigned specimens, probably due to inadequate venting of nitrogen gas from the original specimens. No semi-empirical relations could be derived to fully explain the trends apparent in the data.

The thermal conductivity test results show only a marginal improvement in probe thermal protection performance for a filled honeycomb core compared to an unfilled core. In addition, flatwise tension tests showed a severe bond strength degradation due to the inclusion of either the powder or foam fillers. In view of these results, it is recommended that the baseline OPP design utilize an unfilled core.

1.0 INTRODUCTION

The National Aeronautics and Space Administration proposes to explore the atmospheres of the Outer Planets (Jupiter, Saturn, Uranus and Neptune) using entry probes to perform in situ measurements of the atmospheric structure. The forebody heat protection system is a key element of the probe since it must successfully dissipate the high entry heat loads during the hypersonic entry phase and provide insulation during the longer subsonic descent phase. In the Saturn/Uranus Atmospheric Entry Probe (S/UAEP) study, Reference 1, a baseline heat protection system was selected consisting of a carbon phenolic ablative heat shield bonded to a fiberglass honeycomb (H/C) structural sandwich, Figure 1. During the course of that study, it appeared that first, the high-conductivity hydrogen/helium gases associated with planetary atmospheres would degrade the insulation characteristics of the honeycomb sandwich and second it was desirable for aerodynamic stability to place the equipment just behind the heat shield in order to achieve a forward center of gravity. This in turn implied that the insulation properties of the unfilled honeycomb sandwich should be improved. Packing the honeycomb with a filler material, such as a powder or a foam, represented a conceptual approach for reducing effective gas conductivity of the hydrogen/helium mixture.

FIGURE 1 OUTER PLANET PROBE



The principle of this approach depends on achieving pore sizes within the filler material of the same order as the mean free path of the gas. Under these conditions, a gas molecule is more likely to strike the pore walls rather than another gas molecule resulting in a reduction in the mean free path of the gas. According to kinetic theory this should result in a reduction in the effective gas conductivity. A literature search indicated a lack of insulation conductivity test data in hydrogen or helium environments for the temperatures (300K to 500K) and pressures (up to 10 atmospheres) corresponding to the Reference 1 baseline probe flight environment. Therefore, this test program was undertaken to measure the thermal conductivity for powders and foam under simulated planetary atmospheric environments. These data would then be used to improve the accuracy of the thermal control analysis of the Outer Planets Probe.

Phenolic fiberglass honeycomb specimens 2.54 cm thick with 0.635 cm cell-diameters ($L/D = 4$) were fabricated with the following fillers:

- Unfilled
- 50-50 mixture, carbon black/silica powder (CAB-O-SIL EH-5)
- 50-50 mixture, carbon black/silica powder (CAB-O-SIL MS-7)
- Ultra low density (ULD) silicone elastomeric foam

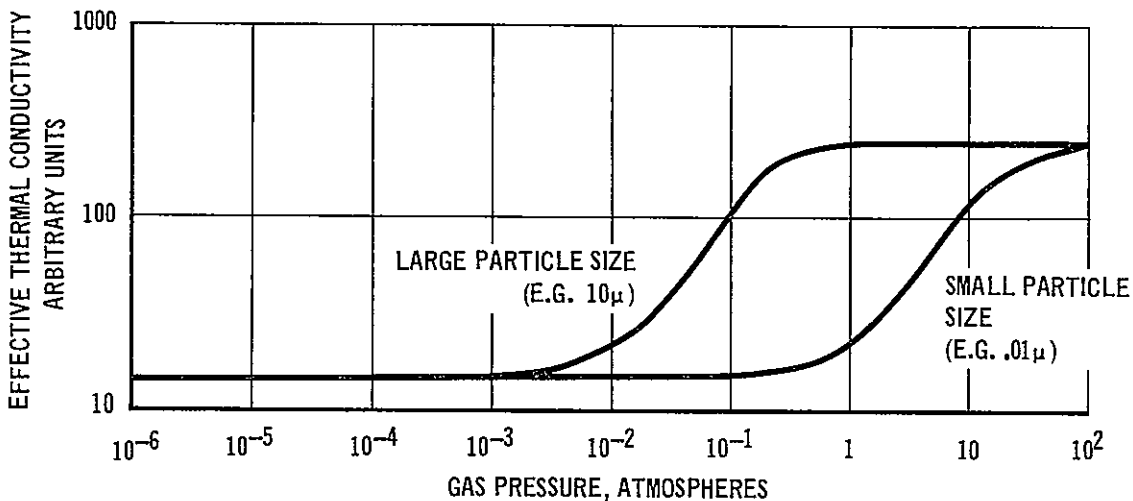
The specimens were tested in helium and in a nitrogen environment to gain a better understanding of the effect of the gas species on the conductivity in a porous medium. In addition, bond strength tests were performed to determine what degradation in bond strength integrity would occur due to the inclusion of the filler material.

After the original test data showed results that could not be fully explained, a new pair of specimens with improved venting characteristics were fabricated and filled with the carbon black/MS-7 filler. The redesigned specimens were tested at an independent laboratory to determine the validity of the original data.

2.0 HEAT TRANSFER IN A POROUS MEDIUM

In general, the thermal energy transport in a porous medium is a combined effect of gas conduction, gas convection, gas-solid conduction, solid contact conduction, and radiation. For medium at moderate temperatures the dominant heat transfer mode is gas conduction. The variation in the conductivity of a porous medium as a function of gas pressure is typically the "S" shaped curve shown in Figure 2, where the breakaway point on the curve is dependent on the medium's pore size and the physical characteristics of the trapped gas. Different investigators have modeled different combinations of the heat transfer modes in deriving analytic correlations for the thermal conductivity in a porous media. In the following paragraphs, various formulations will be presented followed by a discussion of the individual modes of heat transfer.

FIGURE 2 TYPICAL EFFECTIVE THERMAL CONDUCTIVITY OF POROUS MEDIA



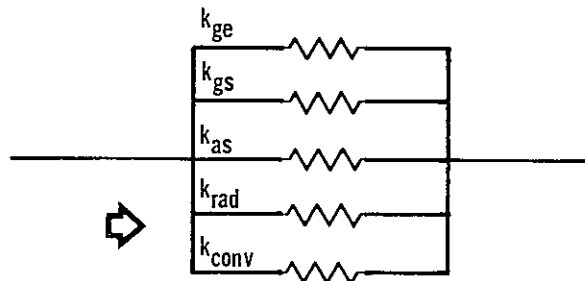
Analytic Models for a Porous Media

To explain the conductivity, many authors have assumed a parallel heat transfer model as depicted in Figure 3, although different authors employ different modes of heat transfer within this model. Vershoor and Greebler, Reference 6, assumed the following form for the thermal conductivity in a fibrous insulation:

$$k = \frac{1}{1-f} (k_{ge} + k_{conv} + k_{rad}) + k_{as} \quad (1)$$

where f is the solid volume fraction of the powder.

FIGURE 3 PARALLEL HEAT TRANSFER MODEL IN A GAS FILLED POWDER BED



In their work, the effective gas conductivity, k_{ge} , was analytically calculated. It was assumed that the net conductivity at minimum pressure was due to solid-solid contact and radiation. k_{rad} was calculated analytically, and k_{as} was taken as the difference at minimum pressure. The apparent convective contribution was assumed to be the difference between the measured data and the sum of the calculated terms.

Johnson and Hollweger, Reference 5, performed an extensive survey of previous work and presented a good treatment of heat transfer in very fine ($\approx .01\mu$) powder mixtures of silica and carbon black at low temperatures. They assumed the following form:

$$k = (1-f)k_{ge} + fk_{gs} + fk_{as} \quad (2)$$

The effective gas conductivity and gas-solid conductivity were determined analytically while k_{as} was taken to be the difference between the theoretical results and the experimental data. Being at low temperatures, radiation contributions were ignored, and convective effects were assumed to be negligible.

A more complete formulation would be a series-parallel model. Dr. John McDonald of Southern Research Institute (SRI), under contract to MDAC-E, formulated the following equation:

$$k = \frac{a k_s k_{ge}}{k_s (1-d) + d k_{ge}} + b k_s + c k_{ge} \quad (3)$$

where a, b, c, and d must be calculated based on the geometry of the model, known void fraction, the conductivity of the powder measured in vacuum, and empirical relations. A more complete explanation of this formulation is presented in Appendix C.

In the following paragraphs, the different modes of heat transfer will be discussed in greater detail, followed by the selection of an appropriate formulation for comparison with the test data.

Effective Gas Conductivity

In the free state, the distance the average molecule travels before a collision (i.e., the mean free path - L_g) is determined by the number of molecules per unit volume. In an enclosure, reducing the gas pressure increases the mean free path, L_g , until eventually L_g is determined by molecular collision with the solid boundaries. Further reductions in pressure have the effect of reducing the gas density without changing the mean free path which would result in a lower thermal conductivity. Early in this century it was suggested that a similar effect would occur by reducing the distance between molecular boundaries rather than reducing the gas pressure. Many investigators, including Reference 4 to 10, have obtained this condition with fine powders, fibers, and foams. Kennard, Reference 11, gives the following relationship for the thermal conductivity of a monatomic gas at low pressures (0.1 torr to 10 atm).

$$k_{g0} = C_p C_v V_a L_g \quad (4)$$

$$L_g = 1 / \sqrt{2} \pi d^2 N_p \quad (5)$$

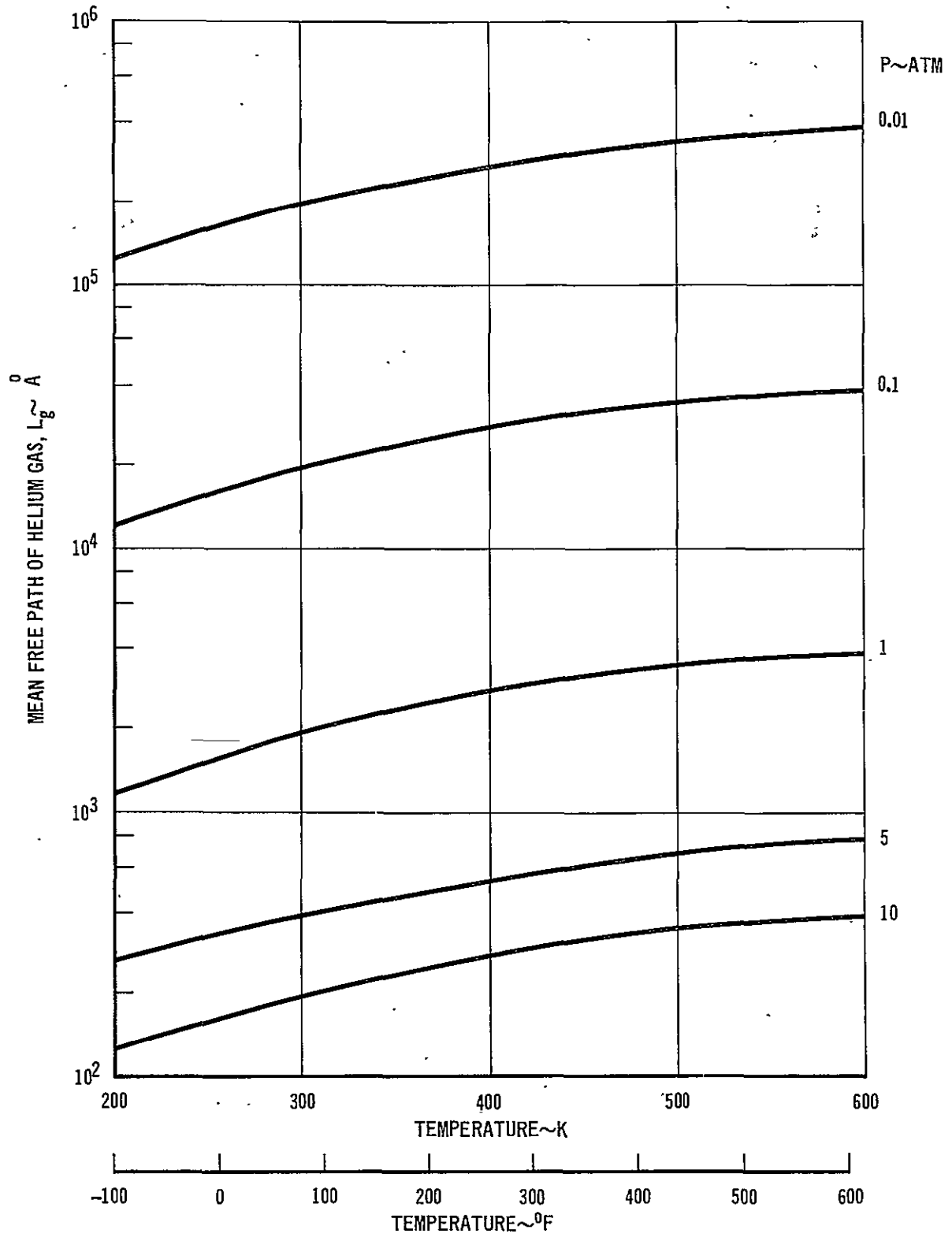
where N_p is the number of molecules per unit volume.

Figure 4 gives values of L_g versus temperature and pressure for helium gas. Appendix A presents the properties of helium and nitrogen gases. Using Equation (4), Equation (3) predicts that k_{g0} is independent of density, and thus is independent of pressure. Reid and Sherwood, Reference 12, show that for both monatomic and diatomic gas molecules of interest, the thermal conductivity varies on the order of 2% from the one atmosphere value over the pressure range of 1 torr to 10 atmospheres.

Verschoor and Greebler derived the following equation for the effective mean free path, L_e , for a gas when constrained in a porous bed

$$L_e = \frac{L_p L_g}{L_p + L_g} \quad (6)$$

FIGURE 4 MEAN FREE PATH OF HELIUM GAS



If it is assumed that the particles are uniform, hard perfect spheres, then L_p can be calculated by:

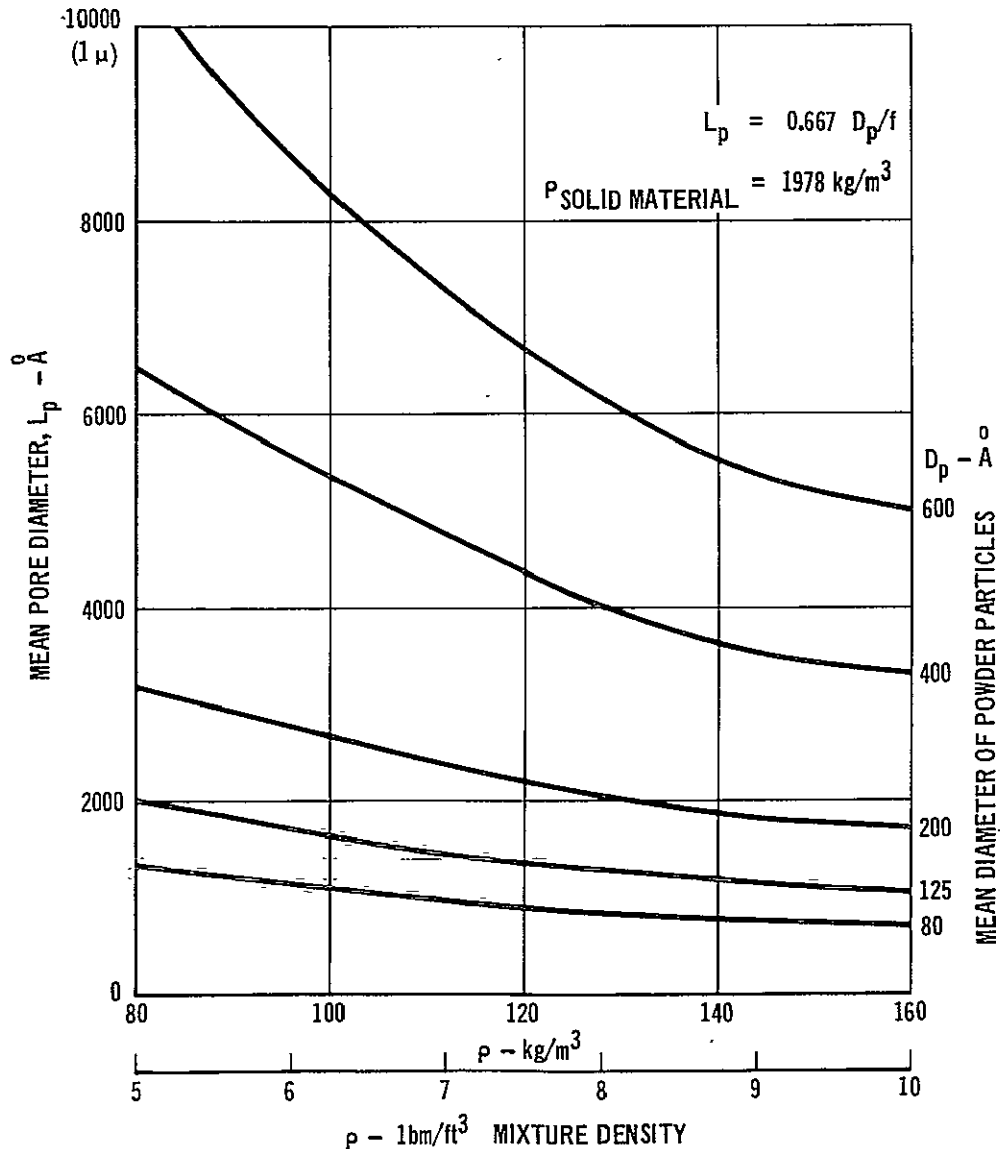
$$L_p = 0.667 \frac{D_p}{f} \quad (7)$$

Figure 5 presents the variations of L_p versus powder density and average particle diameter. The particles in actual commercial powders are not perfect spheres and they tend to form agglomerates. Thus, Equation (6) will underpredict the value of the actual L_p . Substituting L_e for L_g and using Equation (3), they derived the following expression for the effective thermal conductivity of the gas in the packed bed:

$$k_{ge} = k_{go} \frac{L_p}{L_p + L_g} \quad (8)$$

Numerical values for k_{ge} are presented in Section 9.

FIGURE 5 MEAN PORE DIAMETER FOR A 50-50 MIXTURE OF CARBON BLACK AND CAB-O-SIL



Gas-Solid Thermal Conductivity

Johnson and Hollweger give the following equation for the apparent gas-solid thermal conductivity:

$$k_{gs} = \frac{k_{g_0} L_p}{L_p + 2i} \left(\frac{1}{1.f} \right) \quad (9)$$

$$\text{where } i = L_g \left(\frac{2-\alpha}{\alpha} \right) \left(\frac{9\gamma-5}{2(\gamma+1)} \right)$$

Equation (9) represents the heat transfer between the gas and the solid. This equation requires a knowledge of the accommodation coefficient, α , which is a measure of the energy transferred from a gas molecule to a solid surface. Johnson and Hollweger present a good treatment of α , and show why it is very difficult to predict or accurately measure values for α . Typical α values used were 0.35 and 1.0, for helium and nitrogen respectively. Even for $\alpha = 1$ they show that the term fk_{gs} is about two orders of magnitude less than the term $(1.f)k_{ge}$ in their formulation, and thus gas-solid energy transfer would have a negligible influence on the overall conductivity.

Solid Contact Conductivity

An equation for solid contact conductivity, derived by Johnson and Hollweger for their formulations was given as:

$$k_{as} = \frac{6 Y_p}{D_p^2} \quad (10)$$

Y_p was determined experimentally by taking the difference between the test data and the theoretical value of $(1.f)k_{ge} + fk_{gs}$. They state that the actual conductance between the solid spheres is very small, but the conductance along the adsorbed gas layer can be large. For neon and nitrogen which are adsorbed on the surfaces of the fine powder particles, this term amounted to 20-30% of the total conductivity, while for helium, which is not absorbed, only about 2% was attributed to this term. Since this term was experimentally determined, it also included whatever experimental error was present, and was actually a term that was added to explain the difference between their analytic predictions and the test data. In this program, k_{as} will be assumed to be negligible.

Radiation

Radiation transport in an insulation is determined by absorption/reemission, reflection, and scattering by the constituent materials. The radiation contribution is usually given in terms of an equivalent radiation conductivity similar to the approximate expression derived in Section 3. Models exist in the literature, e.g., References 6 through 9, which attempt to model the radiant heat transfer through a porous media. Wechsler, Reference 9, summarizes many of the formulas in the form

$$k_{rad} = C T_m^3 \quad (11)$$

The models that he looked at considered only absorption and reemission, and were applied to insulations with porosities around 70%. Fine powders have porosities of about 95%. Reference 8 presents a treatment of radiation heat transfer in insulations including the effects of backscatter. They conclude that the most efficient means of reducing the radiation for high porosity material is by backscattering rather than absorption/reemission. The maximum backscattering occurs when the particle diameter is about equal to the wavelength of the thermal radiation where the maximum emissive power occurs. For temperatures between 300 K and 500 K, this peak wavelength occurs in the 6μ to 10μ range. If the temperature difference across the insulation is small, Reference 8 presents the following approximate equation:

$$k_{rad} = 4\sigma T_m^3 / N_{bs} \quad (12)$$

where N_{bs} is the backscattering cross section which is a function of the type of material and temperature. Although significant at much higher temperatures, the radiation contribution is expected to be small with respect to k_{ge} with the temperatures measured in this program (e.g., $T < 500$ K).

Natural Convection

None of the references attempted to derive an equation for free convection in a porous medium. Most consider it to be insignificant. Vershoor and Grebler assumed convection to be the difference between the experimental data and the calculated results, but did not derive an analytic expression for it.

In general, free convection is a function of the Rayleigh number as given by

$$Ra = g\beta\Delta TL^3/\nu k \quad (13)$$

In the presence of a porous medium, the free convection contribution is also a function of the permeability of the porous medium, K , as given in the nondimensional Darcy number

$$Da = K/D^2 \quad (14)$$

Just as free convection in a gas initiates at some critical Rayleigh number, Ra_c , free convection in a porous medium initiates at a critical value of the $Da Ra$ product. References 14 through 17 present analysis of free convection in a porous medium. Qualitatively, the added flow resistance due to the filler would delay the onset of natural convection. Below this critical value, the conductivity is assumed to be the thermal conductivity of the gas. As will be shown in Section 3, natural convection should not occur in the helium environment because of the confining dimensions of the H/C core.

Heat Transfer Model in a Porous Medium

The parallel heat transfer model, Figure 3, is a highly idealized model in that it does not take into account interactions between the different modes of heat transfer. As a first approximation, a parallel heat transfer model was assumed since it does offer a simplified model in which each heat transfer term can be examined independently. All the terms in Equations 1 and 2 are small with respect to k_{ge} , and thus both formulations could be reduced to $k = k_{ge}$ in the first approximation. The series-parallel formulation, Equation 3, represents a more accurate formulation of the heat transfer process in a porous medium, but it does contain empirical coefficients. Equation 3 assume that radiation and convection are negligible. This formulation was used later in the program to obtain an improved match with test data.

3.0 HEAT TRANSFER IN A HONEYCOMB CORE

Since the fillers are packed in a H/C core, it is desirable to separate the filler conductivity, k_{Filler} , and the core conductivity, $k_{\text{H/C}}$, for analysis purposes. The thermal conductivity of a honeycomb (H/C) core can be calculated as:

$$k = k_{\text{H/C}} + (1-F) k_{\text{Filler}} \quad (16)$$

where k_{Filler} includes the effects of gas conduction, radiation, etc.

For the empty core, k_{Filler} is the conductivity of the gas, which may include pure conduction or natural convection, plus the radiative contribution, k_{rad} . The radiation contribution can be approximated by assuming two parallel flat plates:

$$Q = \sigma A (T_1^4 - T_2^4) / (1/\epsilon_1 + 1/\epsilon_2 - 1) \quad (17)$$

A radiation heat transfer conductivity can be defined as

$$Q = h_r A (T_1 - T_2) = \frac{k_{\text{rad}}}{L} A (T_1 - T_2) \quad (18)$$

If the temperatures are not too different, this can be expressed as

$$k_{\text{rad}} = 4 \sigma L T_m^3 / (1/\epsilon_1 + 1/\epsilon_2 - 1) \quad (19)$$

The radiation heat transfer in a H/C core is a more complex phenomenon including multiple reflections and radiation to side wall conduction coupling. As a first approximation, the following equation, which was derived from a radiation model of the H/C, can be used to approximate k_{rad} for the H/C core.

$$k_{\text{rad}} = 1.2 \sigma L T_m^3 \quad (20)$$

In an empty honeycomb core, natural convection can have a major impact. For natural convection, the heat transfer coefficient is proportional to the Rayleigh number raised to some power, usually to the 1/4 or 1/3 power depending on whether it is laminar or turbulent convection. The onset of natural convection is dependent on a critical Rayleigh number, Ra_c , which for two horizontal parallel plates heated from below is:

$$Ra_c \approx 1700 \quad (22)$$

Figure 6 presents typical values of Ra_c using expected test conditions. The honeycomb core does restrict the onset of convection currents. References 18 through 21 treat the onset of natural convection in enclosures. In general, as the honeycomb height to diameter ratio (L/D) increases, the value of Ra_c increases. For $L/D = 4$, as is the case for the honeycomb core under study, and perfectly conducting walls, Reference 19 gives $Ra_c = 6 \times 10^5$. Most theoretical analysis has been based on perfectly conducting walls, but Reference 18 gives experimental results for phenolic fiberglass H/C. As shown in Figure 7, lower thermal conductivity walls, e.g., fiberglass, decrease Ra_c for a given L/D value. For values of Ra greater than Ra_c , the heat transfer coefficient, given in the dimensionless Nusselt number (Nu), increases and approaches the parallel plate case in the limit. These results are shown in Figure 8. For a helium environment of 10 atmospheres, a temperature of 300 K, and an $L/D = 4$, the Rayleigh number from Figure 6 is about 10^5 . From Figure 8, we would thus expect no natural convection. Since the inclusion of a porous medium in the H/C would delay the onset of natural convection even further because of the added flow resistance, natural convection would not be expected in a helium environment in the filled H/C core.

FIGURE 6 RAYLEIGH NUMBER FOR VARIOUS GASES

$\Delta T = 40^{\circ}\text{C}$ (ACROSS THE SPECIMEN)

$L = .0254$ METERS

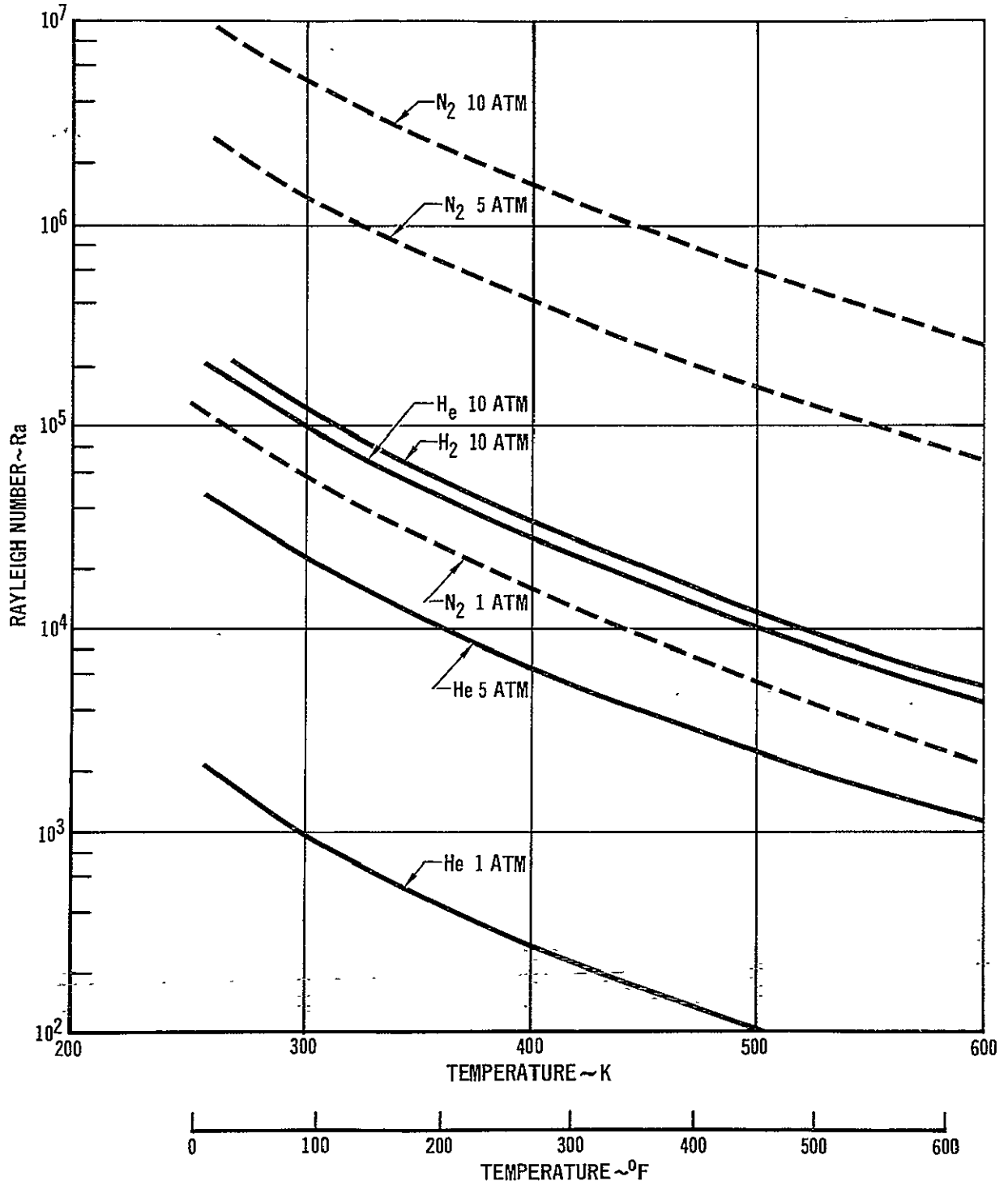


FIGURE 7 ONSET OF NATURAL CONVECTION IN A FIBERGLASS HONEYCOMB CORE HEATED FROM BELOW

- CATTON DATA-PHENOLIC FIBERGLASS (REF. 18 & 19)
- - - - - EXTENSION OF CATTON DATA
- CATTON DATA-ALUMINUM CORE
- - - - - HOLLANDS DATA-THIN WALLED H/C (PERFECTLY CONDUCTIVE) WITH SQUARE CELLS (REF. 20)

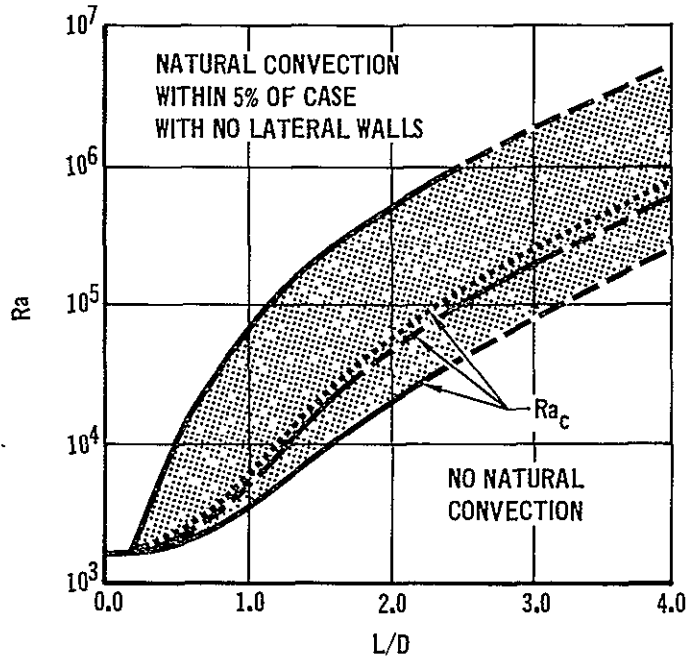
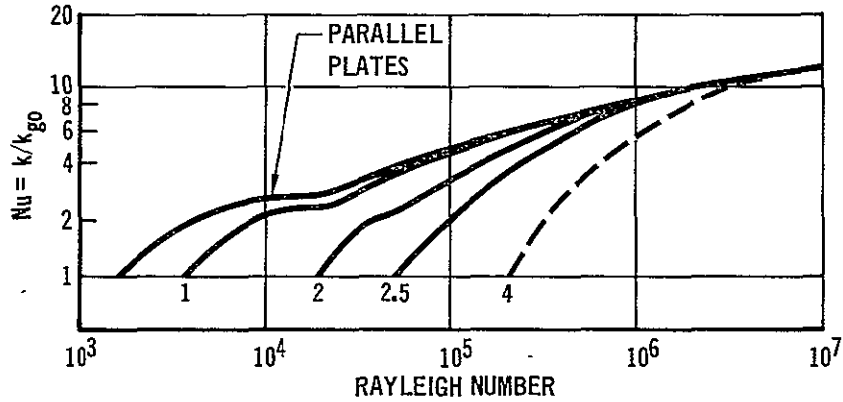


FIGURE 8 HEAT TRANSFER IN A FIBERGLASS HONEYCOMB CORE HEATED FROM BELOW



4.0 SPECIMEN FABRICATION

Figure 9 presents a schematic of the thermal conductivity test specimens. The choice of materials, adhesives, and sizes were based on the OPP honeycomb substructure configuration design presented in Reference 23. Figure 10 shows an unassembled test specimen. Nine thermal conductivity test specimens were fabricated as shown in Figure 11: two unfilled, three filled with EH-5 Cab-O-Sil and carbon black, two filled with MS-7 Cab-O-Sil and carbon black, and two filled with ULD-200-14 syntactic elastomeric foam. Actual thicknesses of the individual parts are presented in Appendix A. The powder filled specimens were prepared by bonding the HRP phenolic/fiberglass honeycomb core to the aluminum face plate with HT-424 adhesive. The powder mixtures were comprised of equal parts by weight of carbon black (Monarch 1100) and Cab-O-Sil which had been mixed in a V-blender, Figure 12, for two hours. A Mylar retainer was taped around the specimen and the core filled with the proper powder mixture such that an 8 cm excess of powder existed on top of the sample. Specimen 4, the first specimen that was made, was prepared by randomly vibrating the fixture. The resulting density was only 70.4 kg/m^3 , which was not acceptable. To achieve a higher powder density, the specimens were agitated by bottom tapping at a rate of 2400 taps per hour. Figure 13 presents a picture of the set-up for packing the powder. The EH-5 powder specimens were tapped for 13 hours each. The two MS-7 powder mixture samples were tapped 13 hours and 24 hours respectively. The volume and weight of the core was measured before tapping. After packing the excess powder was carefully removed and the specimens were again weighed. From this data, the density of the powder in the core was determined. All weights and packed densities are presented in Appendix A. The EH-5 powder mixture attained a maximum density of 5.6 lbm/ft^3 (89.6 kg/m^3), and the MS-7 powder mixture attained a maximum density of 7.8 lbm/ft^3 (124.8 kg/m^3). It should be noted that both of the MS-7 powder specimens packed to the same density although they were tapped for different lengths of time. All tapping was done at one atmosphere pressure with the specimens in a horizontal plane. Higher packing possibly can be attained by packing in a vacuum. The foam filled specimens were prepared by hand pressing a batch of silicone elastomeric foam (ULD-200-14) into the honeycomb. This foam is a low density ablator similar to the type used in the aft cover of the OPP. All specimens were completed by bonding on a phenolic fiberglass face plate with HT-424. The HT-424 adhesive was cured in an autoclave at a temperature of 450 K at 3 atm. pressure, and finally under a full vacuum. The ULD-200-14 material, when used, was cured simultaneously with the HT-424 adhesive during bonding. Specimens 1, 2, and 4 were cured first, and a slight amount of warping was noticed due to the difference in the thermal expansion coefficient between aluminum facesheet and the fiberglass facesheet. Both sides were sanded down to within 0.008 cm. The remainder of the samples were cured in one batch process. After curing, all remaining samples were found to be warped, but to a degree that varied for each specimen. To reduce the surface unevenness, both sides of the samples were sanded to within the limits of the face plate thickness. After sanding, specimens 3, 5, 6, 7, 8 and 9 had a waviness that varied between 0.025 cm and 0.051 cm amplitude. All specimens were shimmed with a rubber pad in the test to provide better interface contact.

There was a concern about whether the honeycomb core would vent properly during the test. Since the conductivity is a function of the gas pressure in the core, the core must have the same pressure as the measured chamber pressure to obtain meaningful data. Specimen 4, which was not used in the test because of its low powder density, was placed in a bell jar, and the jar evacuated. Results indicated that it would take in excess of 30 hours to completely vent the core. To aid venting of the H/C core, sixty 0.066 cm diameter holes were drilled through the fiberglass facesheet of Specimen 4. This directly vents about 10% of the cores. Due to the fineness of the powder, air venting through these holes also carried away some of the powder. To permit venting of the gas but not the powder, a filter composed of two sheets of phenolic fiberglass were attached to the top of the perforated facesheet with RTV-732 adhesive between the vent holes. All test specimens were perforated similarly, and fiberglass filters were added to the four powder filled specimens.

FIGURE 9 SPECIMEN CONFIGURATION

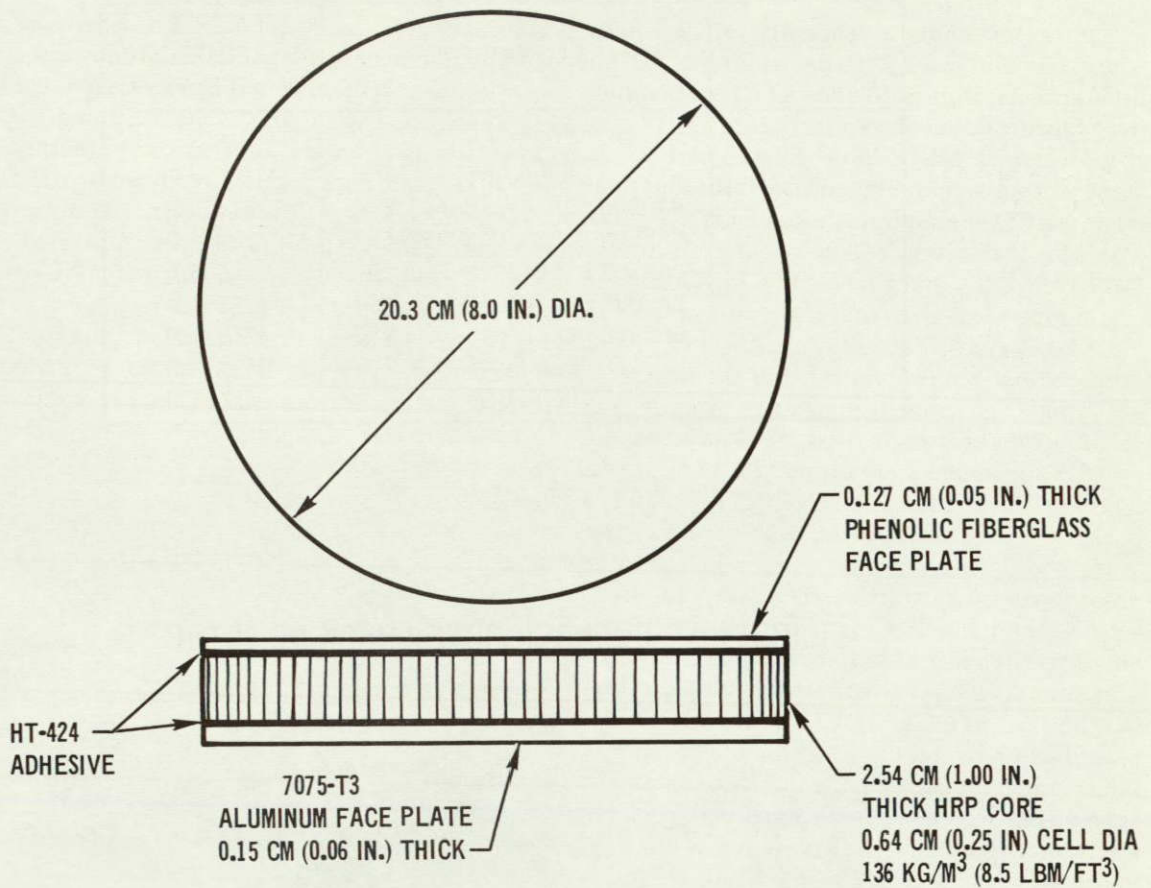


FIGURE 10 UNASSEMBLED TEST SPECIMEN

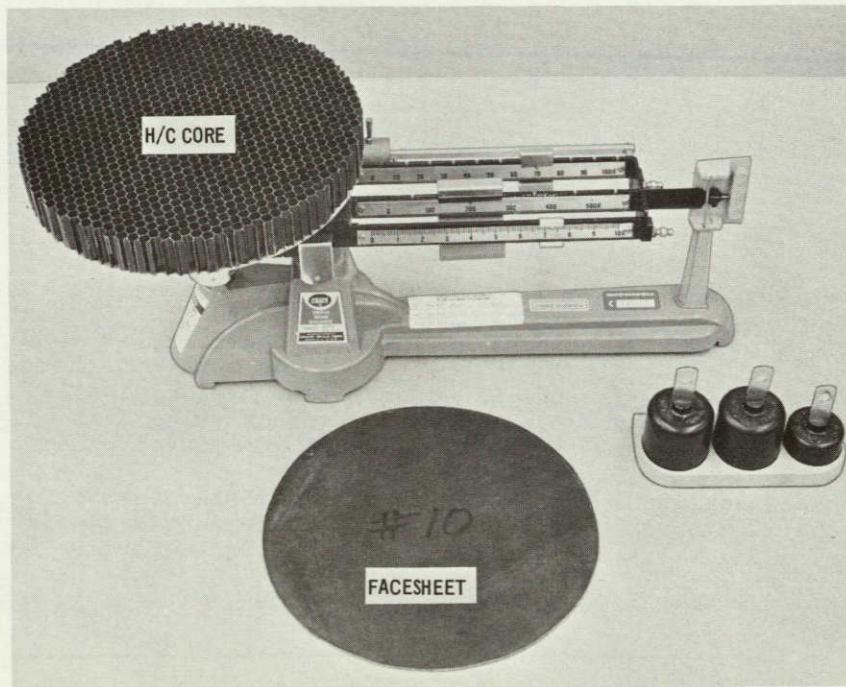


FIGURE 11 SPECIMENS FABRICATED

SPECIMEN NO.	FILLER MATERIAL	MEASURED FILLER DENSITY kg/m ³ (lbm/ft ³)
1	UNFILLED	-
2	UNFILLED	-
3	CARBON BLACK/CAB-O-SIL EH-5	89.6 (5.6)
4	CARBON BLACK/CAB-O-SIL EH-5	70.4 (4.4)
5	CARBON BLACK/CAB-O-SIL EH-5	81.6 (5.1)
6	CARBON BLACK/CAB-O-SIL MS-7	124.8 (7.8)
7	CARBON BLACK/CAB-O-SIL MS-7	123.2 (7.7)
8	ULD FOAM	153.6 (9.6)
9	ULD FOAM	161.6 (10.1)

FIGURE 12 V-BLENDER POWER PACKING SETUP

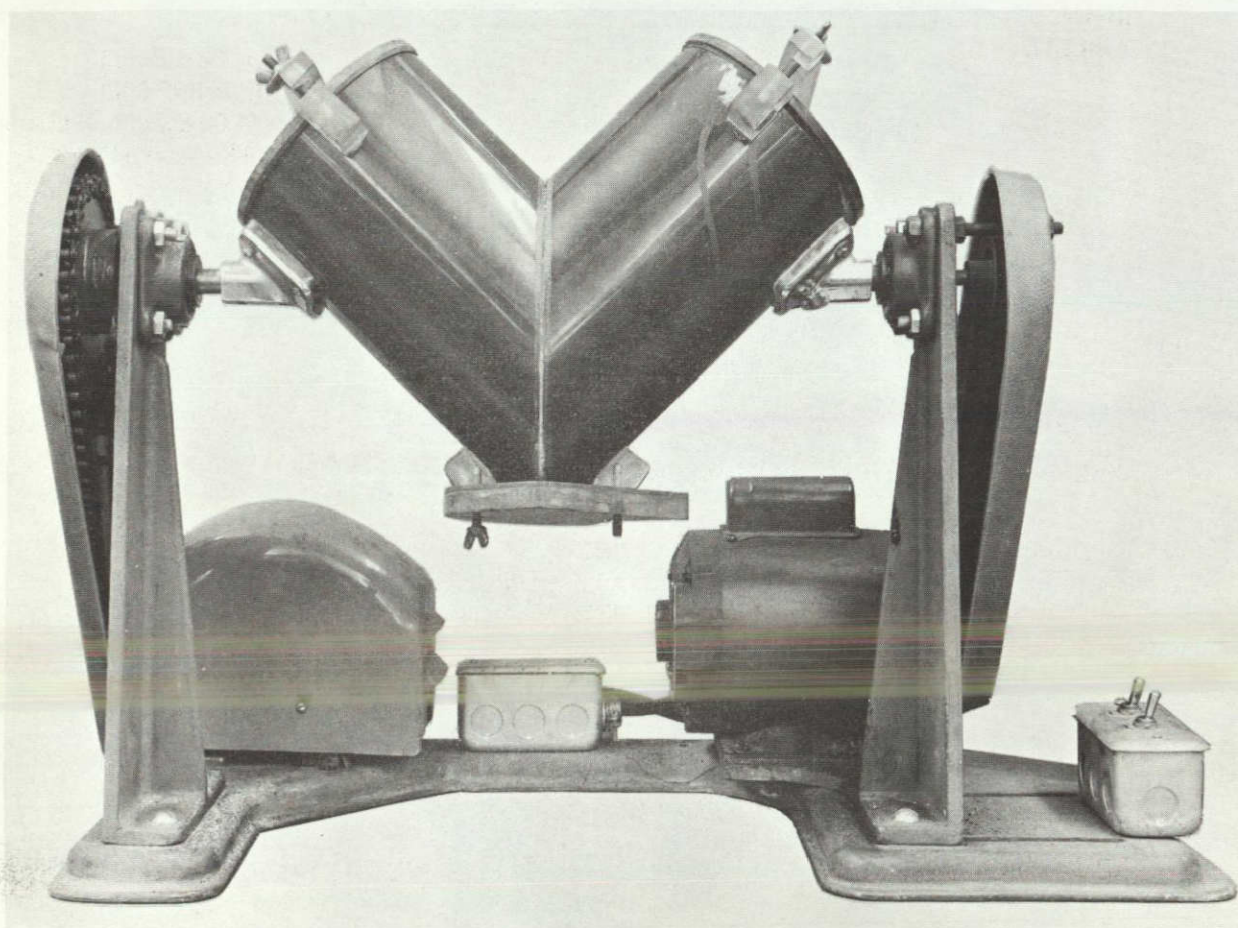
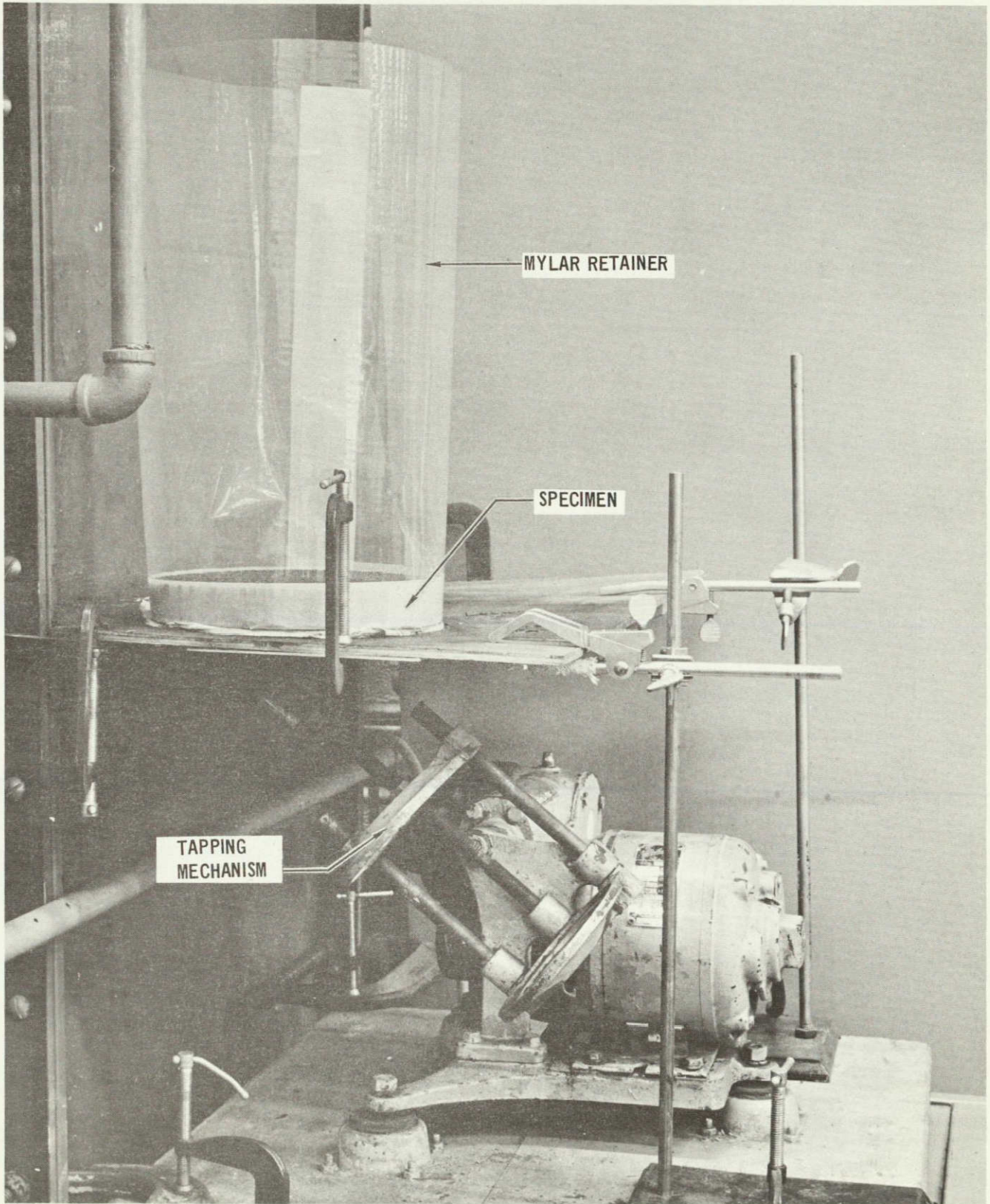


FIGURE 13 SETUP FOR PACKING THE POWDER



5.0 TEST DEFINITION

During entry and descent into the atmospheres of the outer planets, the internal insulation will experience pressures from deep space vacuum up to 10 atm, and will reach temperatures in the 300 K to 600 K range. To determine the best means of reducing the thermal conductivity of the honeycomb substructure insulation, three types of lightweight porous materials were selected for testing. Two types of powder mixtures were selected because of their low density and small mean pore size: a 50-50 mixture by weight of carbon black and two types of silica powder, Cab-O-Sil EH-5 and Cab-O-Sil MS-7 powders. The MS-7 powder has a larger mean particle diameter and packs to a higher density. The two types of silica powders were chosen because the different mean particle diameters and packing densities should yield information on the internal heat transfer mechanism. Carbon black was added, as per Reference 5, in an attempt to reduce the radiation heat transfer while maintaining a small pore diameter. An ultra low density (ULD-200-14) foam was also selected for testing because it has a reasonably small pore size and is easily packed into the H/C core. The physical properties are given in Appendix A.

The atmospheres of the outer planets consist primarily of hydrogen, but testing in a hydrogen environment would present a severe safety hazard. Helium gas, which has very similar thermal properties to hydrogen but which is inert, was chosen as the primary test gas. A limited number of tests were also run in a nitrogen environment in order to gain a better understanding of how the gas properties effect the insulation performance. Although the hot face insulation temperatures may approach 500 K, it was decided to test only up to 483 K because the fiberglass starts to char at about 483 K. To obtain the temperature dependency, specimen mean temperatures of 300 K, 400 K, and 483 K were selected for testing. The testing at 300 K showed that the MS-7 powder mixture had the lowest thermal conductivity, and thus this filler was chosen for testing at higher temperatures to obtain the performance over the entire temperature and pressure range. Since the Reference 1 study had a baseline mission to 10 atm, all candidate insulation concepts were tested from near vacuum conditions to 10 atm pressure. To assess the advantages of using fillers, several runs were made with the unfilled specimens.

Figure 14 identifies the test conditions and specimens for each of the 43 runs. The test case number does not correspond to the actual chronological order in which the tests were run. In general, the order in which the tests were run is:

- a) low pressure, 300 K; He and N₂
- b) high pressure, 300 K; He and N₂
- c) high pressure, 400 K; He
- d) low pressure, 400 K; He
- e) repeated test points; He
- f) 434 K, 483 K, 456 K; He

FIGURE 14 TEST MATRIX

TEST CASE NO.	FILLER MATERIAL	AMBIENT GAS	NOMINAL MEAN TEMPERATURE (K)	NOMINAL PRESSURE (ATM)
1	UNFILLED	He	300	<0.0001
2	UNFILLED	He	300	0.1
3	UNFILLED	He	300	1.0
4	UNFILLED	He	300	5.0
5	UNFILLED	He	300	10.0
6	UNFILLED	N ₂	300	<0.0001
7	UNFILLED	N ₂	300	0.1
8	UNFILLED	N ₂	300	1.0
9	UNFILLED	N ₂	300	5.0
10	UNFILLED	N ₂	300	10.0
11	ULD FOAM	He	300	0.01
12	ULD FOAM	He	300	0.1
13	ULD FOAM	He	300	1.0
14	ULD FOAM	He	300	5.0
15	ULD FOAM	He	300	10.0
16	ULD FOAM	N ₂	300	1.0
17	CARBON BLACK/CAB-O-SIL MS-7	He	300	0.01
18	CARBON BLACK/CAB-O-SIL MS-7	He	300	0.01
19	CARBON BLACK/CAB-O-SIL MS-7	He	300	0.1
20	CARBON BLACK/CAB-O-SIL MS-7	He	300	1.0
21	CARBON BLACK/CAB-O-SIL MS-7	He	300	1.0
22	CARBON BLACK/CAB-O-SIL MS-7	He	300	5.0
23	CARBON BLACK/CAB-O-SIL MS-7	He	300	10.0
24	CARBON BLACK/CAB-O-SIL MS-7	N ₂	300	1.0
25	CARBON BLACK/CAB-O-SIL MS-7	N ₂	300	5.0
26	CARBON BLACK/CAB-O-SIL MS-7	N ₂	300	10.0
27	CARBON BLACK/CAB-O-SIL EH-5	He	300	<0.0001
28	CARBON BLACK/CAB-O-SIL EH-5	He	300	0.1
29	CARBON BLACK/CAB-O-SIL EH-5	He	300	1.0
30	CARBON BLACK/CAB-O-SIL EH-5	He	300	5.0
31	CARBON BLACK/CAB-O-SIL EH-5	He	300	10.0
32	CARBON BLACK/CAB-O-SIL EH-5	N ₂	300	<0.0001
33	CARBON BLACK/CAB-O-SIL EH-5	N ₂	300	0.1
34	CARBON BLACK/CAB-O-SIL EH-5	N ₂	300	1.0
35	CARBON BLACK/CAB-O-SIL MS-7	He	400	<0.0001
36	CARBON BLACK/CAB-O-SIL MS-7	He	400	0.01
37	CARBON BLACK/CAB-O-SIL MS-7	He	400	0.1
38	CARBON BLACK/CAB-O-SIL MS-7	He	400	1.0
39	CARBON BLACK/CAB-O-SIL MS-7	He	400	5.0
40	CARBON BLACK/CAB-O-SIL MS-7	He	400	10.0
41	CARBON BLACK/CAB-O-SIL MS-7	He	434	1.0
42	CARBON BLACK/CAB-O-SIL MS-7	He	456	1.0
43	CARBON BLACK/CAB-O-SIL MS-7	He	483	1.0

6.0 TEST SETUP

The specimen thermal conductivity was measured in the standard guarded hot plate calorimeter apparatus per the procedures in ASTM-C177. A detailed description of the apparatus and procedure is presented in Appendix B. A schematic of the test setup is shown in Figure 15. In general, the guarded hot plate is operated by controlling the heat input to the central heater by adjusting the voltage and current. A differential thermocouple between the central and the guard heater controls the power into the guard heater to minimize the heat loss in the radial direction. This procedure provides for one-dimensional heat transfer through the specimen. On the cold face, a water-cooled cold plate removes the heat. To compensate for the specimen surface unevenness, a rubber filler was placed on the cold side (aluminum) and a fiberglass filler was placed on the hot side (fiberglass). Even with the fillers, perfect contact between the heater surface and the facesheets was not achieved. Since the specimen is vented through the fiberglass facesheet, the use of a thick rubber pad to take out all of the unevenness would not have permitted the specimen to be vented. To improve the accuracy, a direct method for measuring the temperature difference across the specimen was employed, that is, the thermocouples were bonded directly to the test specimen. In the presence of a gas, the gas layer will provide adequate conductance between the heater and the specimen. Two types of coldplates, an unheated and a heated, were employed and are described in Appendix B. Figures 16 and 17 show the test set up with the unheated coldplates. All runs at one atm or less were run in the bell jar. For runs at 5 or 10 atm pressure, a high pressure autoclave was used. Typical test setups in the bell jar and in the autoclave are presented in Figures 18 and 19, respectively. With the unheated coldplate, two tests could be run simultaneously, but the size of the heated coldplate would allow only one test to be run at a time. For a given specimen pair, the same specimen was always placed on the top. For the low pressure testing, the bell jar was evacuated and backfilled to 1 atm with either helium or nitrogen gas. The 1 atm test point was run first followed by the lower pressure tests. On the average, all the low pressure tests stabilized within 12 to 24 hours. In the high pressure testing, the autoclave was evacuated, refilled with the desired gas, evacuated again, and refilled to the desired pressure. All high pressure tests were stabilized within 8 hours.

FIGURE 15 TEST SETUP

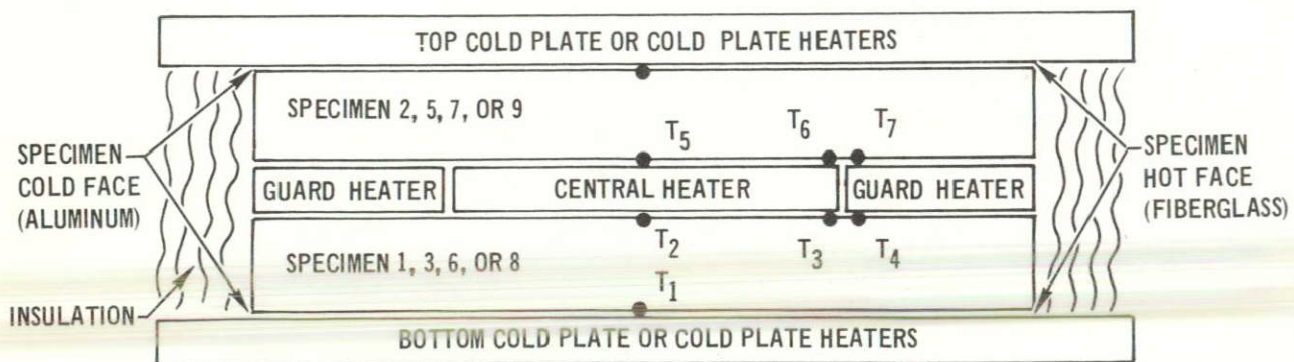


FIGURE 16 THERMAL CONDUCTIVITY TEST STACK WITH UNHEATED COLDPLATES

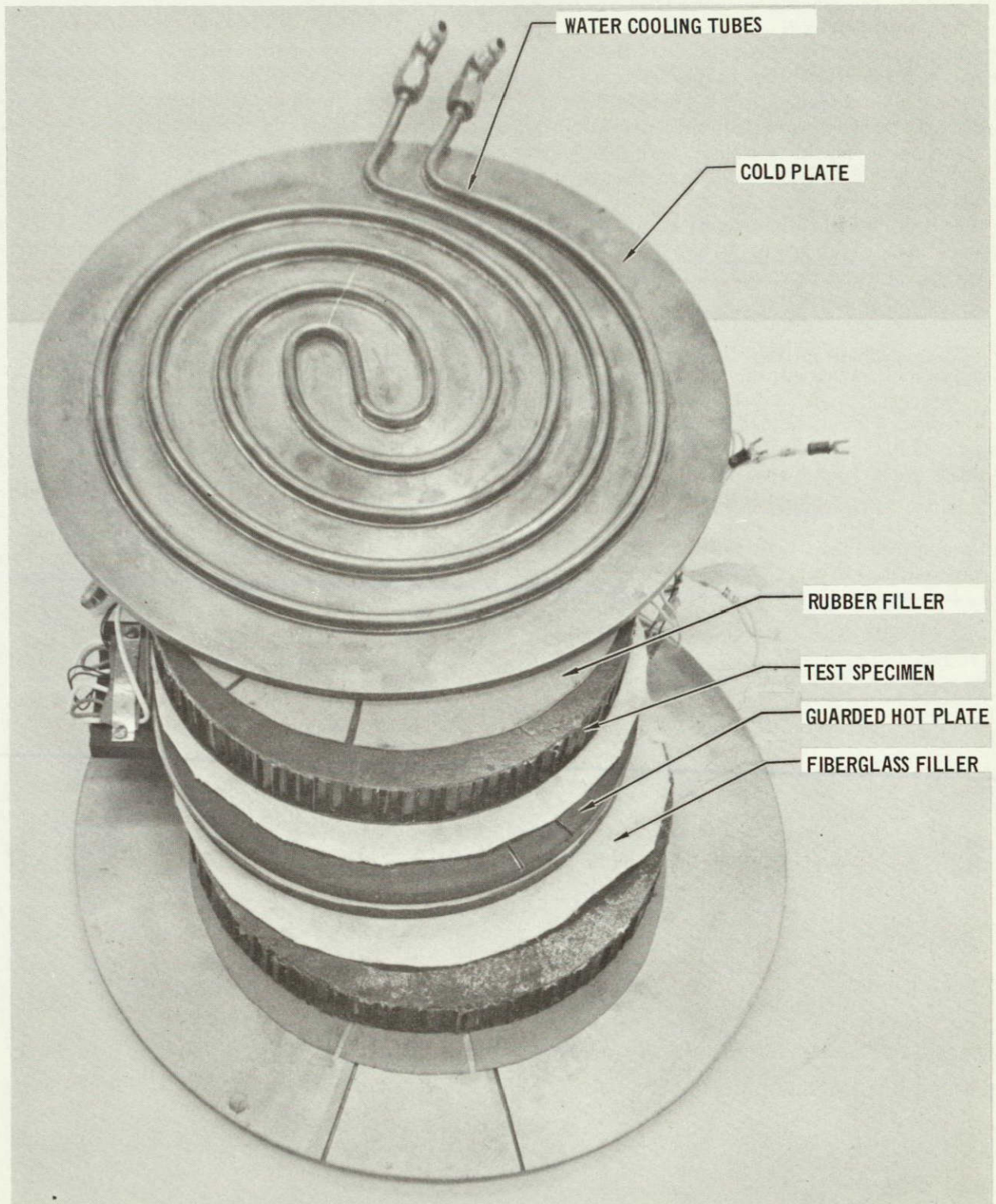
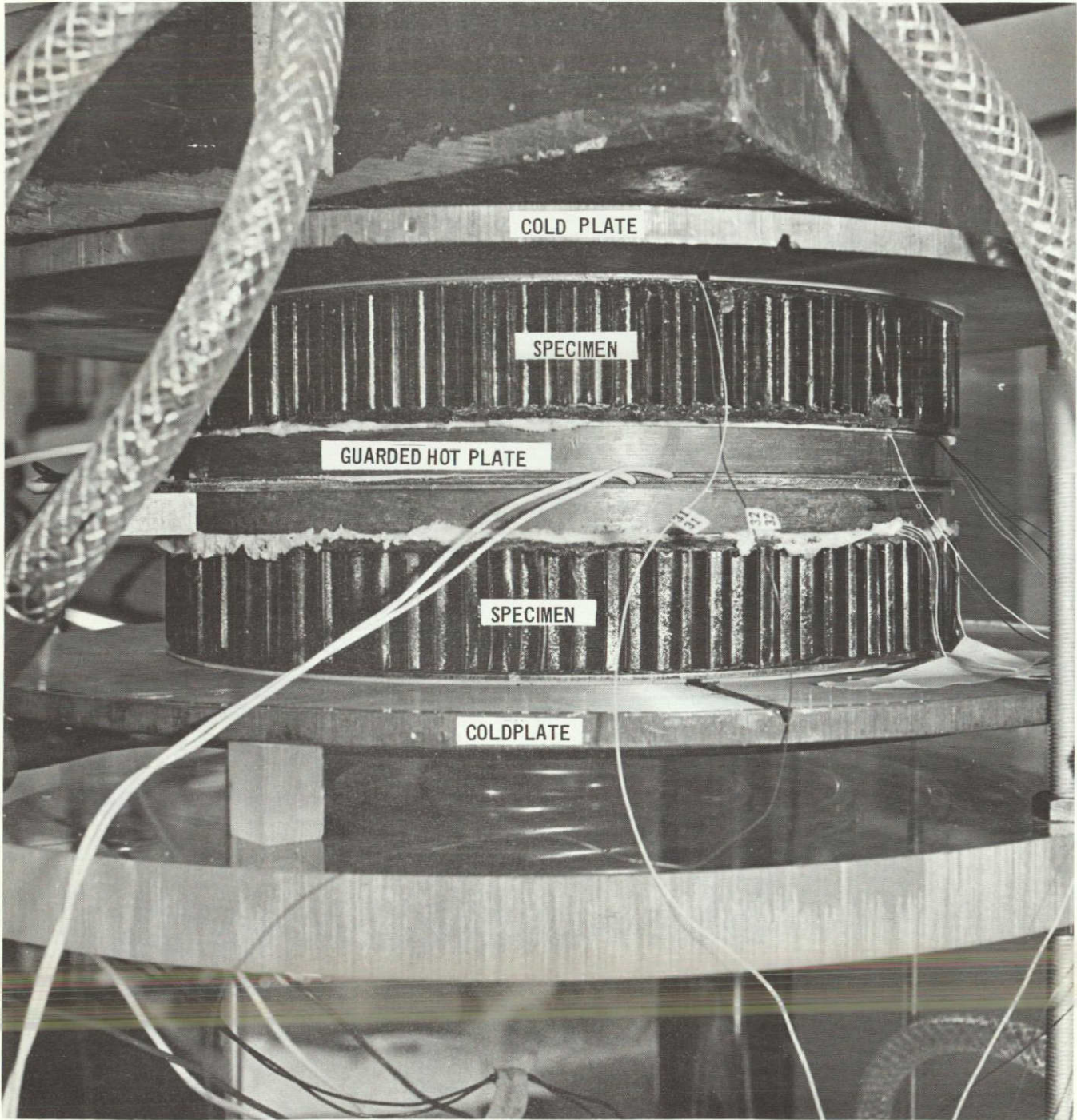


FIGURE 17 ASSEMBLED TEST STACK



**FIGURE 18 TWO GUARDED HOTPLATE CALORIMETER SETUPS
INSTALLED IN A VACUUM BELL JAR**

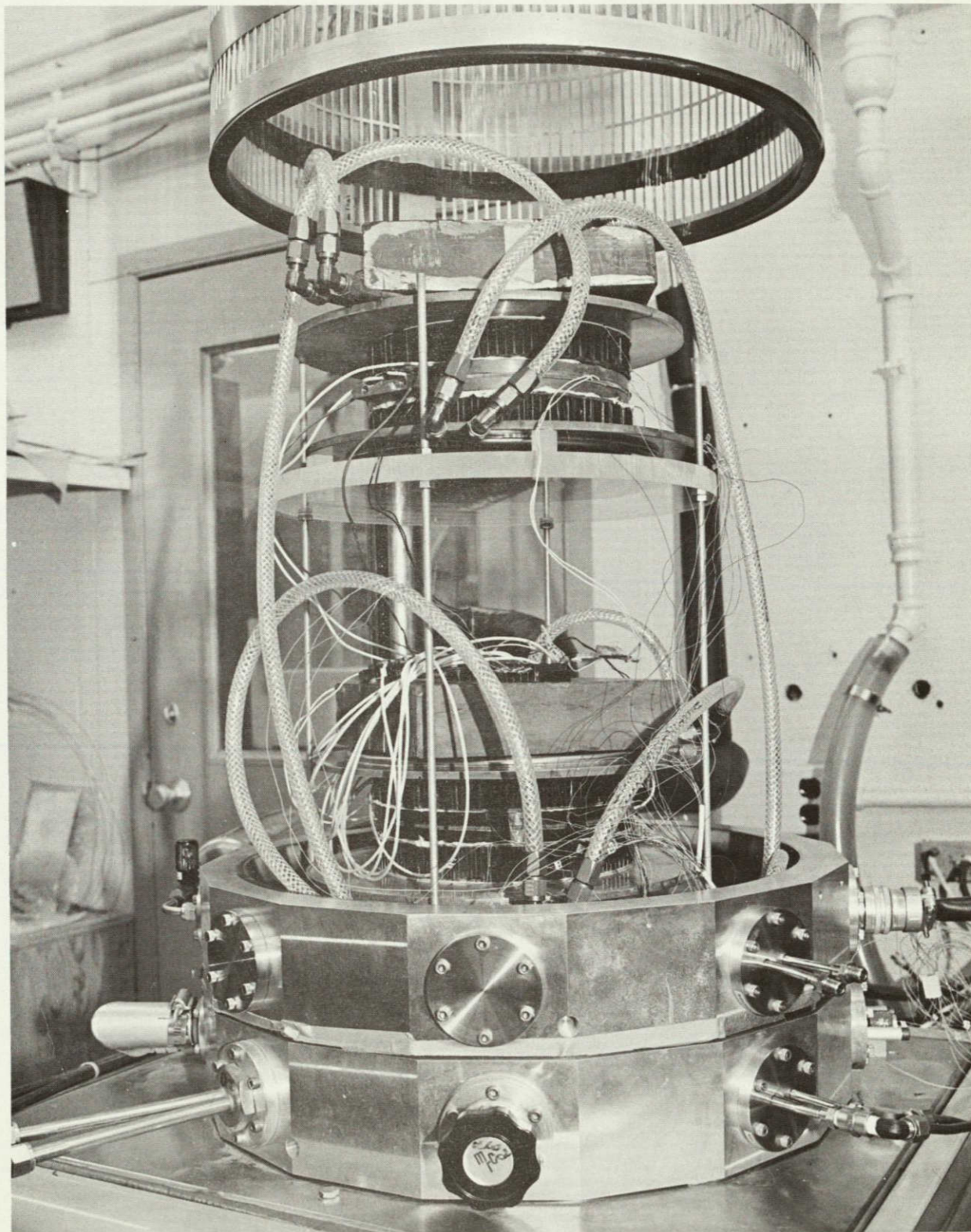
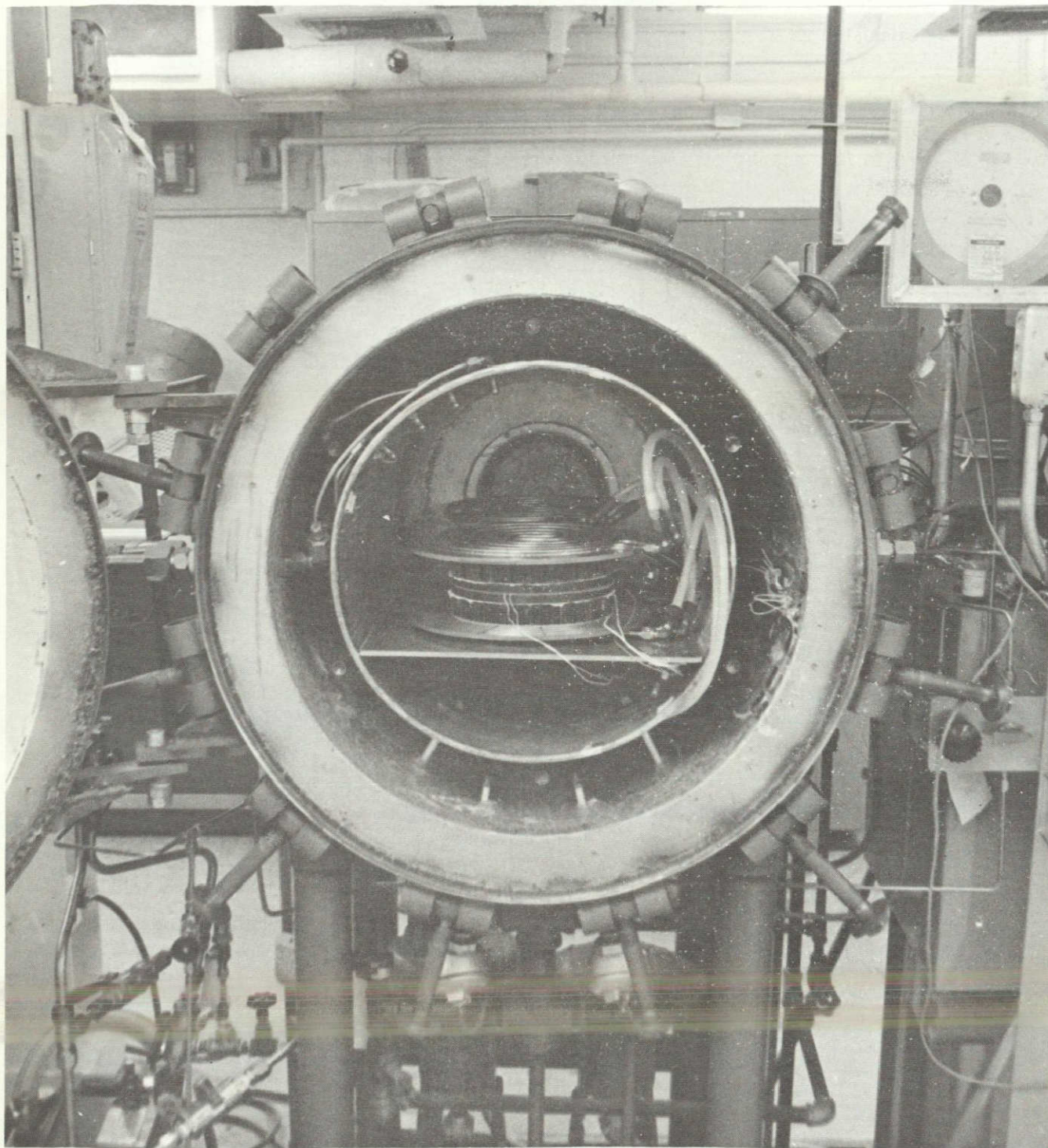


FIGURE 19 TWO GUARDED HOTPLATE CALORIMETERS IN A HIGH PRESSURE AUTOCLAVE



7.0 TEST RESULTS

The temperature, voltage, and current measurements for each thermal conductivity test are presented in Figure 20. The one dimensional heat transfer through the specimen is given by:

$$Q = \frac{kA}{L} \Delta T \quad (23)$$

Thus, k can be calculated as

$$k = QL/A\Delta T \quad (24)$$

For the guarded hot plate calorimeter that was used, $A = 0.008108 \text{ m}^2$. The specimen thickness was taken to be the thickness of the honeycomb core ($L = 0.0254 \text{ m}$). The power added to the central heater, Q_{total} , is assumed to flow equally between the two specimens. Thus, k can be calculated as:

$$k = \frac{Q_{\text{total}}}{2} \frac{0.0254}{0.0081 \Delta T} = 1.566 \frac{Q_{\text{total}}}{\Delta T} \quad (25)$$

Where $Q_{\text{total}} = \text{volts} \times \text{amperes}$ and ΔT is in K

As described in Section 3, the thermal conductivity of the specimen, assuming a parallel heat transfer model, is the sum of the H/C and the filler conductivity

$$k = k_{\text{H/C}} + (1-F) k_{\text{Filler}} \quad (26)$$

The conductivity of the filler is thus:

$$k_{\text{Filler}} = \frac{k - k_{\text{H/C}}}{1-F} = \frac{k - k_{\text{H/C}}}{0.924} \quad (27)$$

When measuring the conductivity of an empty H/C core, solid conduction, gas conduction or convection, and radiation contribute to the heat transfer. When the cells are filled with a fine powder at near vacuum conditions and low temperatures, the gas conduction and radiation contributions become very small when compared to the solid conduction through the H/C core ribbon material. Thus the honeycomb conductivity, $k_{\text{H/C}}$, was taken to be the conductivity of the powder-filled specimen at the near vacuum conditions. Data were available on the thermal conductivity of phenolic fiberglass measured perpendicular to the layers and these data is presented in Figure 21. In the powder-filled core, the fiberglass ribbon has layers parallel to the heat flow, and additional small conduction contribution fo solid contact conduction and radiation. Unfortunately, the high temperature vacuum test point (test run no. 35), was run with the specimens that had appreciable warp, and without the conductive gas layer the results appeared to be low. To obtain values of $k_{\text{H/C}}$, the value at $T = 300 \text{ K}$ was extended to higher temperatures using the same slope as the previous phenolic fiberglass data. These values were then used in Equation 27 to determine k_{filler} . The values of the thermal conductivity from these tests are presented in tabular form in Figure 22. The results of the tests in the nitrogen environment are plotted in Figure 23, and the results in the helium environment are plotted in Figure 24.

The results from test case 17 were not consistent with the rest of the data. This run was terminated after about 6 hours, and thus probably did not reach equilibrium. A rerun of this test point was made and a more consistent data were obtained. To insure the repeatability of the data, test case number 20 was repeated just prior to the 434 K test point but after all of the 400 K test points had been run. The results, test case 21, was the same as test case number 20.

FIGURE 20 TEST DATA



TEST CASE NO.	TEST PRESSURE	T ₁ K(°F)	T ₂ K(°F)	T ₅ K(°F)	T ₈ K(°F)	CENTRAL VOLTS	HEATER POWER AMPERE
1	1.3 x 10 ⁻⁵ TORR	282.6(49.4)	316.0(109.4)	313.8(105.5)	283.5(51.0)	2.688	0.384
2	77 TORR	281.0(46.4)	316.6(110.5)	316.0(110.0)	280.3(45.2)	5.734	0.79
3	753 TORR	280.8(46.2)	320.5(117.6)	320.4(117.3)	280.3(45.0)	6.206	0.86
4	5.0 ATM	283.1(44.8)	322.2(120.6)	322.3(120.8)	280.0(44.7)	6.925	0.88
5	10.0 ATM	280.2(45.1)	328.9(132.6)	328.7(132.3)	280.9(46.3)	7.469	0.94
6	1.0 x 10 ⁻⁵ TORR	281.7(48.7)	313.3(104.6)	311.0(100.5)	283.0(50.1)	2.887	0.413
7	76 TORR	280.3(45.2)	315.7(109.0)	315.2(108.1)	280.0(44.6)	3.484	0.484
8	750 TORR	280.1(44.8)	316.4(110.2)	315.3(108.2)	280.1(44.8)	3.453	0.492
9	5.0 ATM	280.2(45.1)	319.2(115.3)	323.1(122.2)	281.6(47.6)	5.648	0.710
10	10.0 ATM	280.1(44.9)	318.5(113.9)	314.9(107.4)	282.6(49.3)	6.121	0.770
11	7.6 TORR	277.9(40.9)	321.0(118.4)	321.0(118.5)	277.5(40.2)	4.390	0.55
12	76 TORR	277.9(40.9)	315.4(108.3)	315.4(108.4)	277.5(40.2)	4.667	0.59
13	752 TORR	278.8(42.6)	321.6(119.6)	321.6(119.6)	278.4(41.8)	5.683	0.71
14	5.0 ATM	280.1(44.9)	318.9(114.7)	318.5(114.0)	280.0(44.7)	5.960	0.825
15	10.0 ATM	280.3(45.2)	320.2(117.0)	319.8(116.3)	280.5(45.5)	6.162	0.85
16	752 TORR	278.8(42.6)	320.6(117.7)	320.1(116.9)	278.6(42.2)	3.613	0.456
17	7.6 TORR	277.2(39.7)	325.4(126.3)	325.3(126.2)	277.1(39.5)	3.870	0.52
18	8.0 TORR	288.1(59.3)	339.2(151.2)	339.2(151.2)	287.0(57.3)	3.445	0.44
19	76 TORR	277.1(39.4)	324.2(124.2)	324.4(124.5)	277.1(39.4)	3.854	0.53
20	752 TORR	278.2(41.4)	331.5(137.3)	331.6(137.6)	278.0(41.1)	5.056	0.70
21	741 TORR	291.1(64.6)	332.5(139.2)	332.5(139.2)	290.3(63.2)	4.776	0.58
22	5.0 ATM	279.2(43.3)	321.1(118.7)	321.1(118.7)	279.6(43.9)	5.556	0.77
23	10.0 ATM	280.0(44.7)	323.8(123.5)	323.9(123.6)	280.4(45.4)	5.958	0.825
24	752 TORR	278.1(41.3)	331.0(136.4)	331.1(136.6)	278.6(42.1)	3.281	0.469
25	5.0 ATM	279.7(44.1)	331.1(140.3)	333.1(140.3)	280.1(44.8)	3.895	0.53
26	10.0 ATM	279.6(44.0)	327.3(129.8)	327.5(130.1)	279.6(44.0)	3.838	0.52
27	1.3 x 10 ⁻⁵ TORR	281.0(46.5)	316.2(109.9)	315.6(108.8)	282.6(49.4)	2.339	0.295
28	77 TORR	279.6(44.6)	321.2(118.9)	321.2(118.9)	279.9(44.5)	4.464	0.56
29	753 TORR	280.5(45.5)	333.5(141.0)	333.5(140.9)	280.3(45.2)	6.159	0.78
30	5.0 ATM	279.5(43.7)	321.9(120.0)	322.0(120.2)	279.7(44.2)	5.943	0.75
31	10.0 ATM	279.7(44.2)	323.0(122.1)	323.2(122.4)	280.0(44.7)	6.214	0.78
32	1.0 x 10 ⁻⁵ TORR	280.9(46.3)	315.9(109.2)	315.6(108.8)	282.5(49.1)	2.384	0.30
33	76 TORR	280.1(44.9)	322.1(120.3)	322.1(120.5)	280.1(44.9)	3.209	0.410
34	750 TORR	280.2(45.1)	320.1(116.9)	321.1(118.6)	280.3(45.2)	3.477	0.438
35	4.1 x 10 ⁻⁵ TORR	385.9(235.3)	413.3(284.6)	413.6(285.1)	367.2(201.6)	2.172	0.274
36	9.7 TORR	384.1(232.1)	420.4(257.4)	420.5(297.5)	387.8(238.7)	3.233	0.409
37	75.2 TORR	379.4(223.5)	418.9(294.6)	419.0(294.8)	381.2(226.8)	4.619	0.560
38	744 TORR	378.0(227.1)	422.2(300.6)	422.2(300.7)	379.5(232.7)	6.087	0.750
39	5.0 ATM	378.7(222.3)	413.9(285.7)	415.4(288.4)	383.6(231.1)	6.582	0.805
40	10.0 ATM	378.4(221.7)	411.6(281.5)	413.2(284.4)	386.3(236.0)	6.618	0.81
41	733 TORR	414.4(286.6)	451.9(354.1)	451.9(354.1)	414.5(286.8)	6.012	0.74
42	757 TORR	439.6(331.9)	470.1(386.7)	470.3(387.1)	440.9(334.2)	6.066	0.75
43	744 TORR	470.0(386.3)	496.8(434.8)	496.7(434.7)	466.9(381.1)	6.466	0.80

△ THERMOCOUPLE READINGS ARE ACCURATE TO ±1°F, BUT WAS CONVERTED AND RETAINED TO THE NEAREST .1 K THROUGHOUT THE CALCULATIONS

FIGURE 21 H/C CORE CONDUCTIVITY

$f = 0.076$

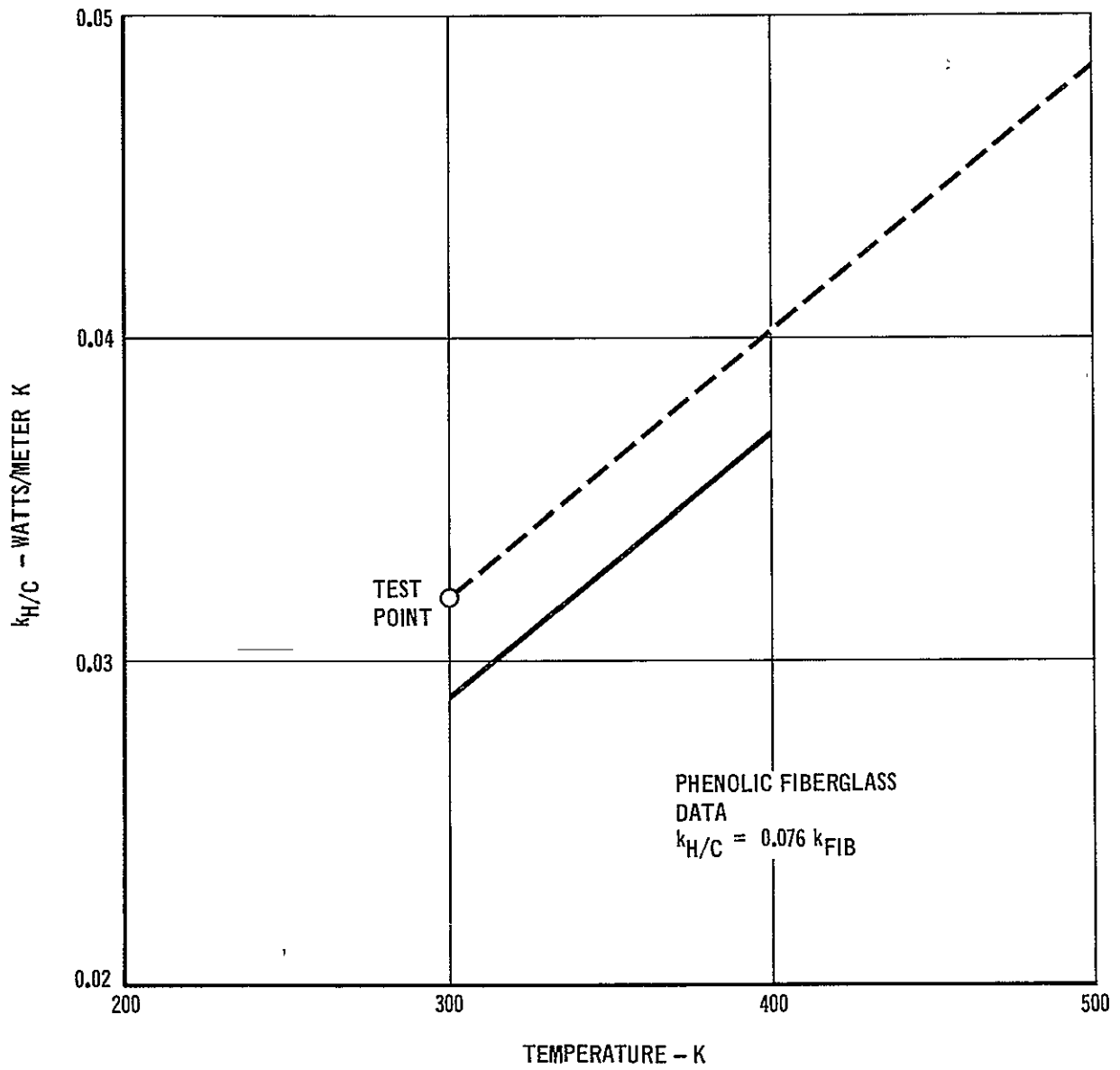


FIGURE 22 THERMAL CONDUCTIVITY TEST RESULTS

TEST CASE NO.	FILLER	SPECIMEN NO.	GAS	NOMINAL PRESSURE (ATM)	NOMINAL MEAN TEMPERATURE K	THERMAL CONDUCTIVITY WATTS/METER/ K			
						k _{TOTAL}	k _{FILLER}	k _{FILLER} /k _{go}	
1	UNFILLED	1,2	He	<0.0001	300	.051	.021	0.14	
2	UNFILLED	1,2	He	0.1	300	.198	.180	0.20	
3	UNFILLED	1,2	He	1.0	300	.210	.193	1.27	
4	UNFILLED	1,2	He	5.0	300	.226	.210	1.40	
5	UNFILLED	1,2	He	10.0	300	.228	.212	1.41	
6	UNFILLED	1,2	N ₂	<0.0001	300	.040	.009	0.35	
7	UNFILLED	1,2	N ₂	0.1	300	.068	.039	1.50	
8	UNFILLED	1,2	N ₂	1.0	300	.068	.039	1.50	
9	UNFILLED	1,2	N ₂	5.0	300	.156	.134	5.15	
10	UNFILLED	1,2	N ₂	10.0	300	.209	.192	7.39	
11	ULD FOAM	8,9	He	0.01	300	.087	.060	0.40	
12	ULD FOAM	8,9	He	0.1	300	.114	.089	0.59	
13	ULD FOAM	8,9	He	1.0	300	.159	.137	0.91	
14	ULD FOAM	8,9	He	5.0	300	.199	.181	1.21	
15	ULD FOAM	8,9	He	10.0	300	.207	.189	1.26	
16	ULD FOAM	8,9	N ₂	1.0	300	.062	.033	1.27	
17	MS-7 POWDER	6,7	He	0.01	300	(.065)			⚠
18	MS-7 POWDER	6,7	He	0.01	300	.046	.015	0.10	⚠
19	MS-7 POWDER	6,7	He	0.1	300	.068	.039	0.26	
20	MS-7 POWDER	6,7	He	1.0	300	.104	.078	0.52	
21	MS-7 POWDER	6,7	He	1.0	300	.104	.078	0.52	⚠
22	MS-7 POWDER	6,7	He	5.0	300	.161	.140	0.93	
23	MS-7 POWDER	6,7	He	10.0	300	.176	.156	1.04	
24	MS-7 POWDER	6,7	N ₂	1.0	300	.046	.015	0.58	
25	MS-7 POWDER	6,7	N ₂	5.0	300	.061	.031	1.19	
26	MS-7 POWDER	6,7	N ₂	10.0	300	.065	.036	1.39	
27	EH-5 POWDER	3,5	He	<0.0001	300	.032	--	--	
28	EH-5 POWDER	3,5	He	0.1	300	.095	.068	0.45	
29	EH-5 POWDER	3,5	He	1.0	300	.142	.119	0.79	
30	EH-5 POWDER	3,5	He	5.0	300	.165	.144	0.96	
31	EH-5 POWDER	3,5	He	10.0	300	.176	.156	1.04	
32	EH-5 POWDER	3,5	N ₂	<0.0001	300	.033	--	--	
33	EH-5 POWDER	3,5	N ₂	0.1	300	.048	.017	0.65	
34	EH-5 POWDER	3,5	N ₂	1.0	300	.059	.029	1.12	
35	MS-7 POWDER	6,7	He	<0.0001	400	(.016)			⚠
36	MS-7 POWDER	6,7	He	0.01	400	.060	.022	0.12	
37	MS-7 POWDER	6,7	He	0.1	400	.105	.070	0.39	
38	MS-7 POWDER	6,7	He	1.0	400	.164	.134	0.75	
39	MS-7 POWDER	6,7	He	5.0	400	.248	.225	1.26	
40	MS-7 POWDER	6,7	He	10.0	400	.279	.259	1.46	
41	MS-7 POWDER	6,7	He	1.0	434	.185	.154	0.82	
42	MS-7 POWDER	6,7	He	1.0	456	.238	.209	1.09	
43	MS-7 POWDER	6,7	He	1.0	483	.286	.259	1.30	

- ⚠ BAD TEST POINT
- ⚠ REPEATED TEST POINTS
- ⚠ BAD TEST POINT DUE TO UNEVENNESS IN THE SAMPLES
- ⚠ CONDUCTIVITY CALCULATIONS BASED ON THE H/C CORE THICKNESS

FIGURE 23 SPECIMEN THERMAL CONDUCTIVITY DATA IN A NITROGEN ENVIRONMENT

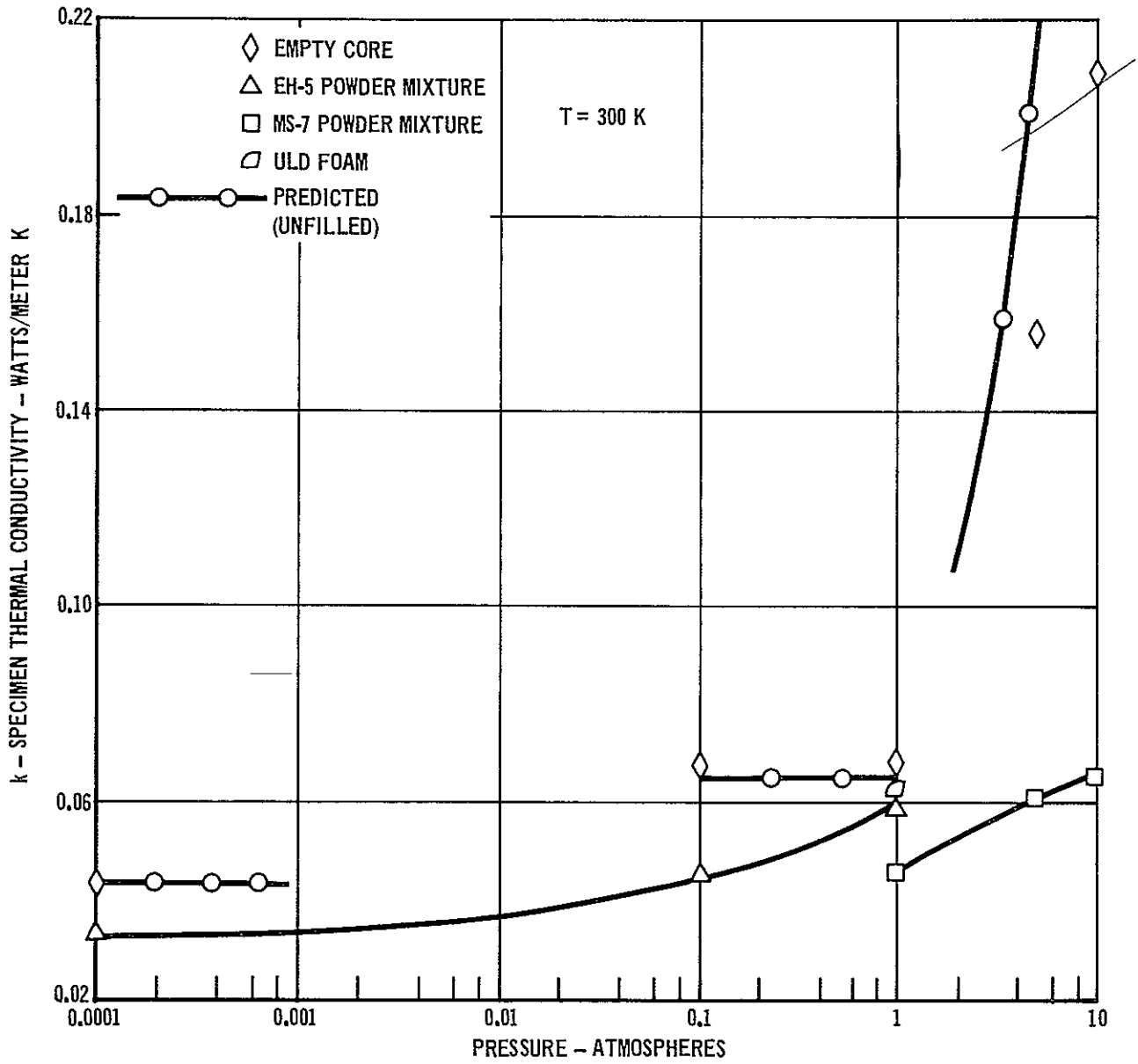
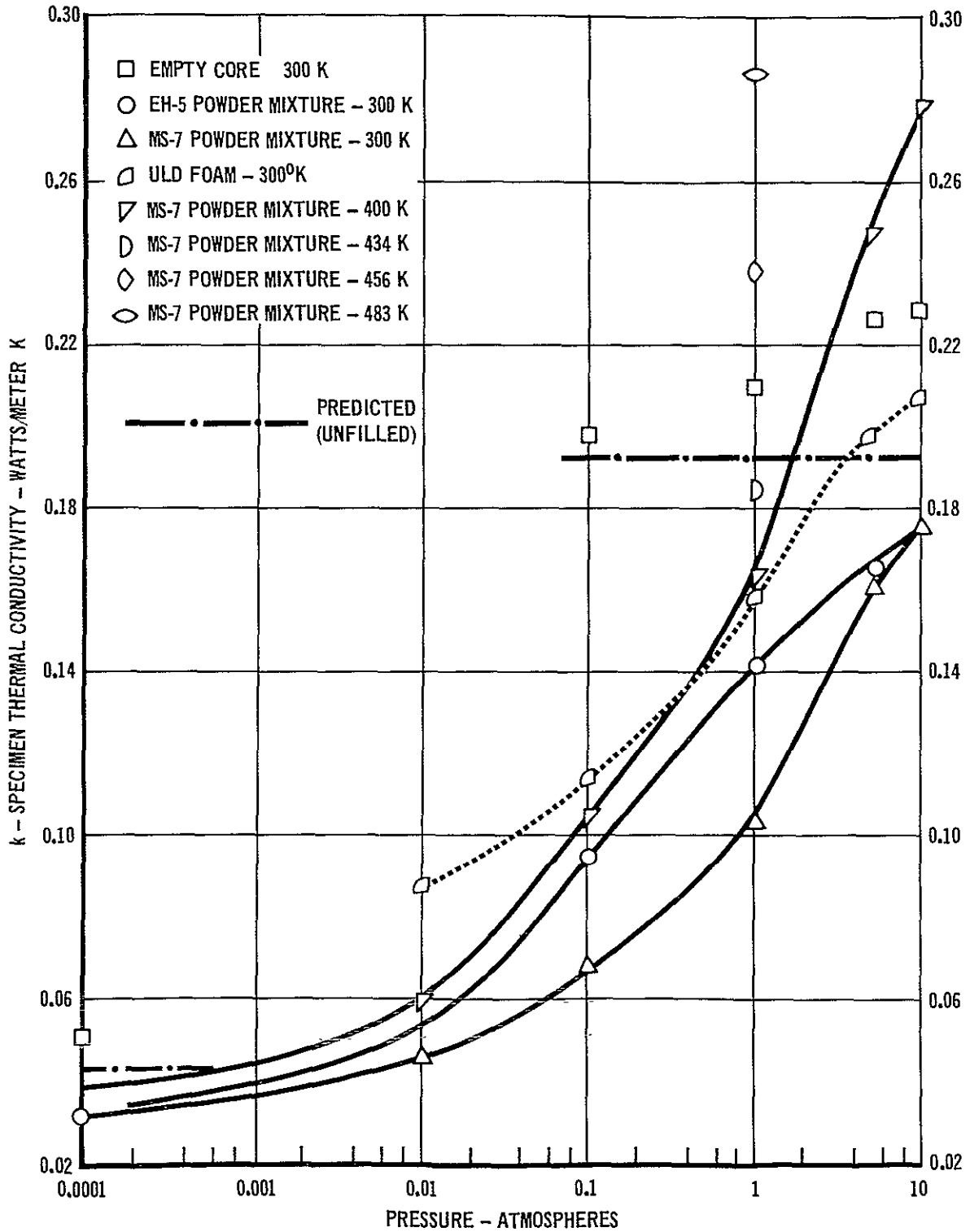


FIGURE 24 SPECIMEN THERMAL CONDUCTIVITY IN A HELIUM ENVIRONMENT



8.0 BOND STRENGTH TEST

Tests were conducted to determine the effect of the filler material on the adhesive bond strength. Three test samples, as shown in Figure 25, were cut from the empty core specimen, the ULD filled specimen, and the EH-5 powder filled specimen. A flatwise tension test, as depicted in Figure 26, was run for each of the nine samples. The test data of these tests are shown in Figure 27. In all cases, the specimens failed at the fiberglass facesheet interface which was the bond made after the filler was added. A summary of the average results are shown in Figure 28, and indicate a severe bond strength degradation due to the inclusion of the filler material. Since the ULD samples had been heated to elevated temperatures, a correction factor was applied to account for the temperature degradations. Based on the results of these tests, none of the concepts that were tested are acceptable fillers for the OPP unless different processes can be found to increase the structural integrity of the bond.

FIGURE 25 FLATWISE TENSION TEST SPECIMEN

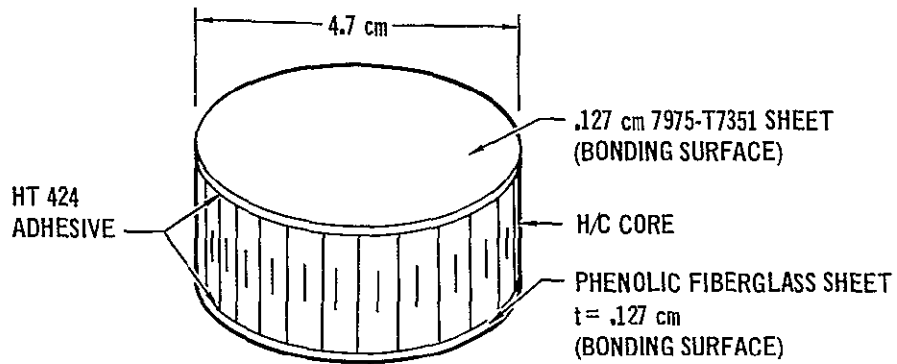


FIGURE 26 FLATWISE TENSION TEST SETUP

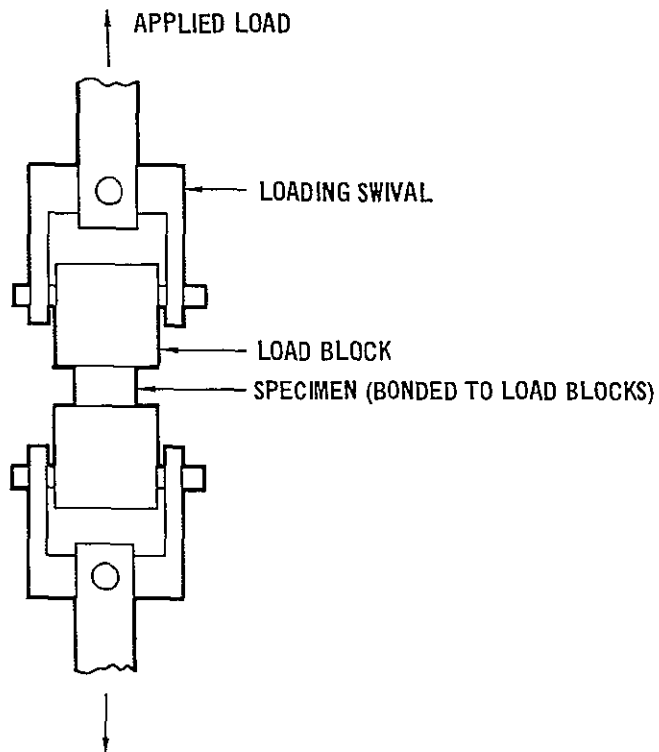


FIGURE 27 FLATWISE TENSION TEST DATA

SPECIMEN	SAMPLE	$F_{tu} - N/m^2$ (PSI)
UNFILLED	1	3.08×10^6 (446.56)
	2	3.04×10^6 (440.69)
	3	3.08×10^6 (446.56)
POWDER FILLED	P1	1.90×10^5 (27.57)
	P2	1.49×10^5 (21.69)
	P3	3.78×10^5 (54.90)
ULD FILLED	U1	5.45×10^5 (79.1)
	U2	5.67×10^5 (82.3)
	U3	6.06×10^5 (88.0)

FIGURE 28 FORWARD HONEYCOMB CORE FLATWISE TENSION TEST RESULTS

SPECIMEN	F_{TU} AVG RESULTS N/m^2 (PSI)	% OF STRENGTH OF UNFILLED
UNFILLED	3.1×10^6 (445)	100
POWDER FILLED	2.4×10^5 (35)	8
ULD FILLED	$*7.6 \times 10^5$ (111)	25

*TEST AVG/.75 TO COMPENSATE FOR HEAT SOAK

9.0 DISCUSSION OF TEST DATA

The conductivity apparatus utilized in this test program is a standard apparatus. However, there were some unique features of this test program that may have introduced some errors and these items are discussed in subsequent paragraphs. Since aluminum has a very high thermal conductivity compared to the core, the temperature drop across the aluminum facesheet of the specimen will be very small. The fiberglass facesheet was sanded to within the limits of the thickness to eliminate high spots, resulting in a thickness variation across each specimen. Since the vast majority of the temperature drop is across the core, all thermal conductivity calculations were based on the 2.54 cm (1 in.) mean core thickness. Since the thermocouples were bonded directly to the specimen, any gap between the heater and the specimen should have little effect on the ΔT across the specimen. As long as there is a gas layer to conduct the heat from the heater to the specimen, the calculated values should be good. The radial heat flow is minimized by the guard heaters as described in Appendix B. On the hot face (fiberglass side) of each specimen, there were three thermocouples radially placed as shown in Figure 15. A summary of the readings for selected runs are presented in Figure 29. If there is a significant error introduced by the unevenness in the samples, it should show up in the radial temperature distributions. As is shown, there is no significant temperature difference between T_1 and T_2 or T_5 and T_6 , which indicates that there is an even heat flux.

FIGURE 29 RADIAL TEMPERATURE DISTRIBUTION
TEMPERATURE - K*

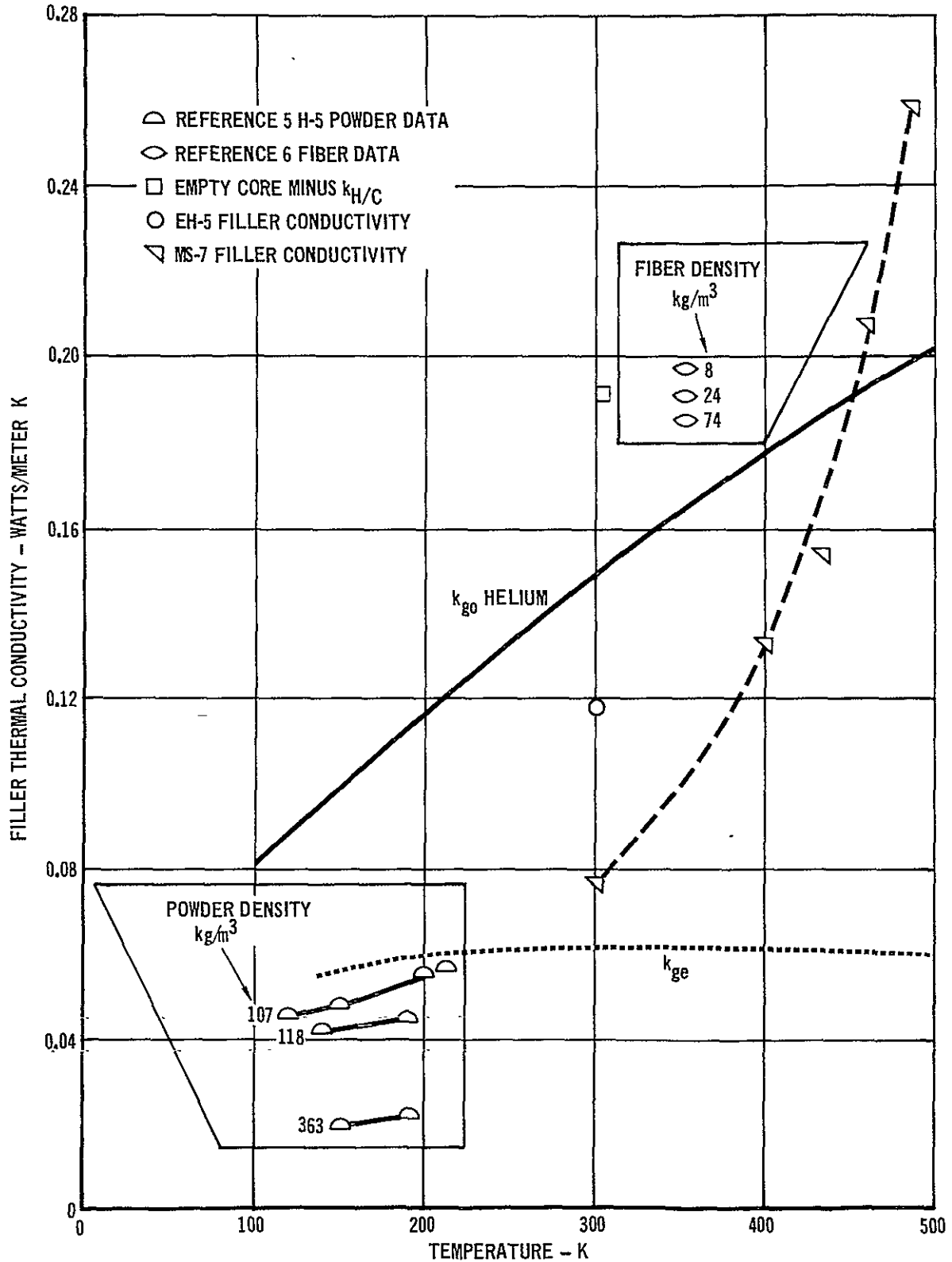
RUN NUMBER	T_1	T_2	T_3	T_5	T_6	T_7
18	339.3	339.3	339.3	339.2	339.2	339.5
19	324.2	324.2	323.8	324.4	324.3	324.1
21	331.5	331.5	331.1	331.7	331.7	331.5
22	321.2	320.6	320.5	321.2	321.0	321.1
23	323.8	323.2	323.0	323.9	323.7	323.7
28	321.3	320.9	320.7	321.3	320.9	320.7
29	333.6	333.1	331.9	333.5	333.0	332.7
36	427.5	428.1	429.6	428.2	428.1	429.3
38	422.2	422.2	421.2	422.3	422.4	421.8
39	413.9	415.2	413.8	415.4	415.4	414.8
40	411.6	412.7	411.4	413.2	413.2	412.6
42	470.1	470.1	468.7	470.3	470.3	469.4
43	496.8	496.8	494.9	496.7	496.7	495.6

*SEE FIGURE 15 FOR T/C LOCATIONS

Examining the empty core data (Figure 23), it is noted that there is a definite increase in conductivity with pressure. Using the Rayleigh number from Figure 6, and the fiberglass H/C data extended for $L/D = 4$ from Figure 8, the test results for the 5 and 10 atm cases for nitrogen fall below the predicted values as shown in Figure 23. Since there is natural convection, appreciable differences in the thermal conductivity between the top and bottom specimens can be expected. This difference will result in errors in the conductivity measurements, with the experimental data indicating values below the actual conductivity of the top specimen. The one atm case for nitrogen agrees with the predicted value. For the helium environment, the Rayleigh number approaches Ra_c for a $L/D = 4$ fiberglass H/C core, which should result in little or no contribution from natural convection. The data indicate a slight rise in conductivity with pressure, with the one atm case about 10% above the predicted value.

Much of the previous data have been generated in a one atmosphere environment. Figure 30 presents the Reference 5, Reference 6 and the current data for the powder filled conductivity as a function of temperature in a one atm helium environment.

FIGURE 30 THERMAL CONDUCTIVITY IN A HELIUM ENVIRONMENT AT ONE ATMOSPHERE PRESSURE USING THE ORIGINAL SPECIMEN DESIGN



Figures 30 through 32 present comparisons of the test data to analytic predictions for k_{ge} . Values for k_{ge} were calculated using the equations in Section 2 and the actual test conditions. There is obviously poor correlation between the data and k_{ge} .

FIGURE 31 COMPARISON OF EXPERIMENTAL RESULTS FOR THERMAL CONDUCTIVITY OF MS-7 POWDER MIXTURE IN A HELIUM ENVIRONMENT

TEMP K	P ATM	k_{ge}	WATTS/METER K	
			k_{FILLER}	$k_{FILLER} - k_{ge}$
300	0.01	0.001	0.015	0.014
300	0.10	0.009	0.039	0.030
300	1.	0.061	0.078	0.017
300	5.	0.116	0.140	0.024
300	10.	0.131	0.156	0.025
400	0.01	0.001	0.022	0.021
400	0.10	0.009	0.070	0.061
400	1.	0.061	0.134	0.073
400	5.	0.128	0.225	0.097
400	10.	0.149	0.259	0.110
434	1.	0.060	0.154	0.094
456	1.	0.060	0.209	0.149
483	1.	0.059	0.259	0.200

In addition, according to Equation 7, both the MS-7 and the EH-5 powder mixtures should have resulted in the same k_{ge} since they both have the same theoretical average pore size. Figure 24 shows an appreciable difference between the two powders. The EH-5 powder is known to form agglomerates more readily which could account for some of the differences.

Using Equation 20, the effective radiation conductivity without the filler or the H/C core was calculated as a function of temperature and is plotted in Figure 33. At higher temperatures, radiation could be a predominant term. It was thought that the silica powder with the carbon black would eliminate any significant contributions due to radiation. Because of a lack of good data in a vacuum at the higher temperatures, the magnitude of the radiation contribution could not be separated from the other heat transfer mechanisms. An IR transmissivity test was run on a 1 cm thick specimen of the MS-7/CB mixture. This test showed that there was no radiation heat transfer through the powder, and thus the large rise in conductivity with temperature cannot be attributed to radiation.

As stated previously, according to available data, there should be little natural convection in an empty H/C core in a helium environment for the conditions tested. Since the introduction of a porous medium would further delay the onset of convection, natural convection would not be expected to have a significant influence on the effective conductivity through the powder bed in a helium environment. For helium and nitrogen gases, the total effective conductivity due to natural convection decreases with increasing mean temperature. To illustrate the point, a curve for the effective conductivity for natural convection between two parallel plates at 10 atm in a helium environment as a function of the mean temperature is presented in Figure 33. Thus, natural convection is apparently not the mechanism that is causing the trends in the data.

As stated previously, neither gas-solid-thermal conductivity or solid contact conductivity could result in the magnitude of the experimental data.

FIGURE 32 COMPARISON OF EXPERIMENTAL DATA
TO ANALYTICAL VALUES OF k_{ge} AT 300 K

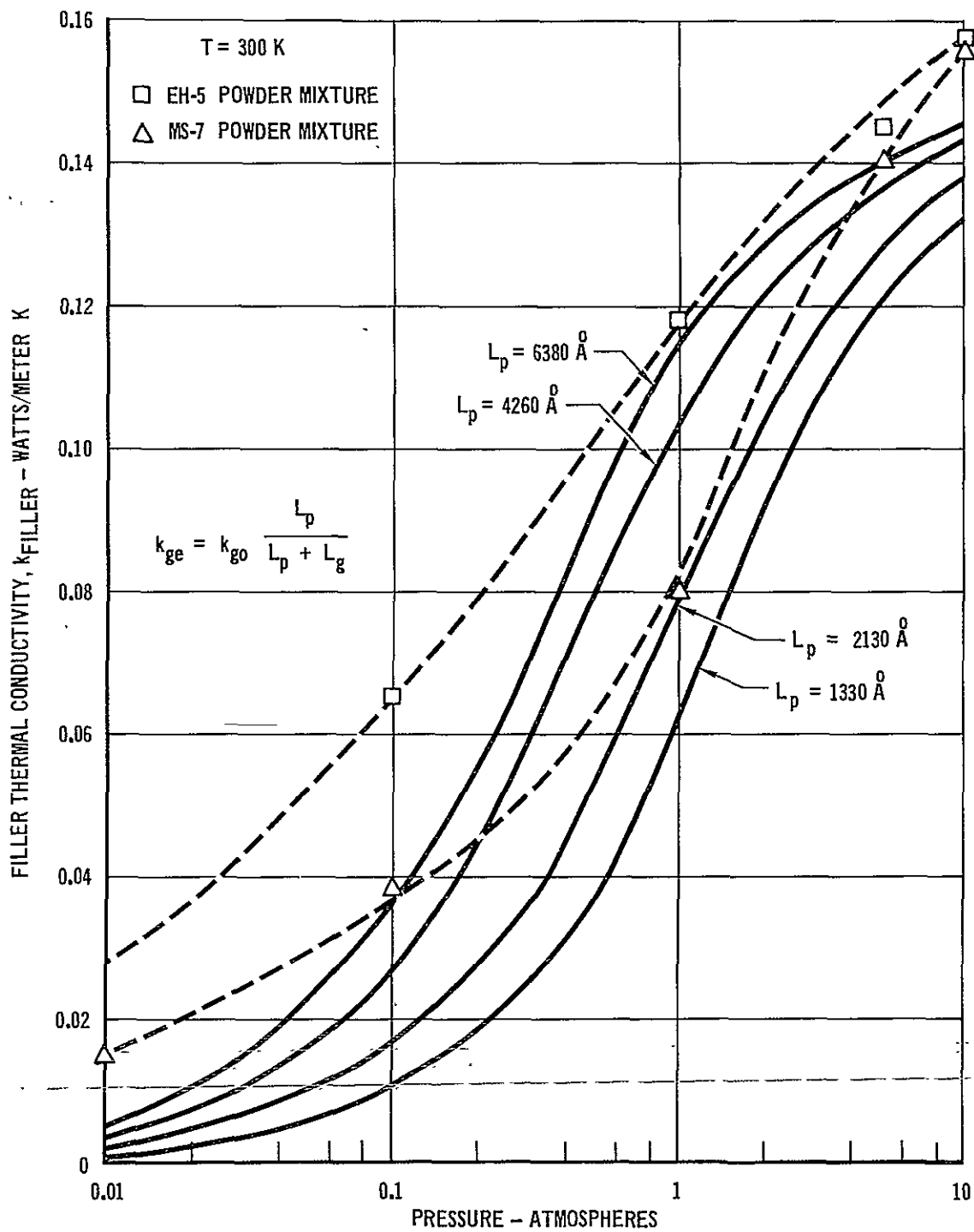
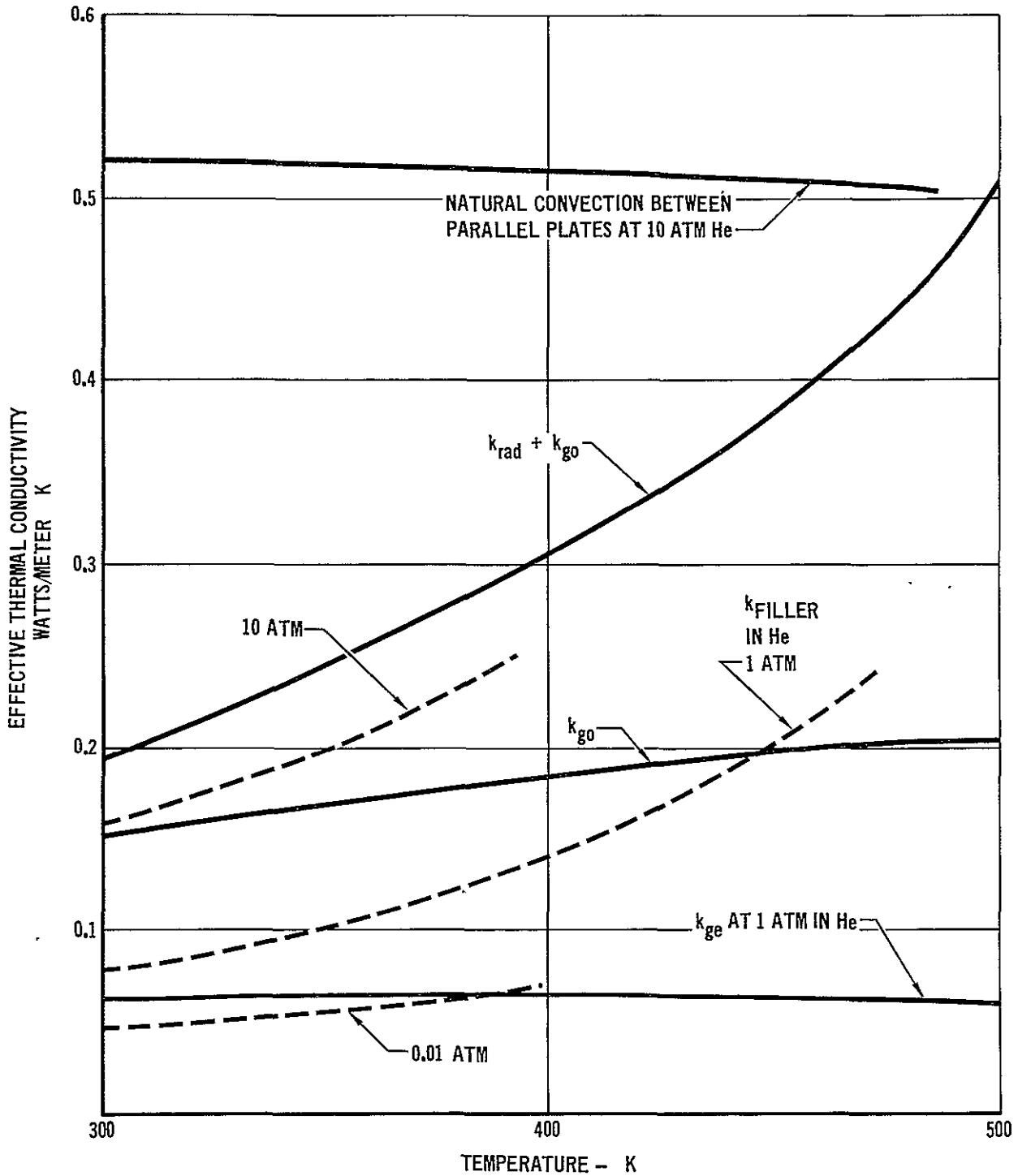
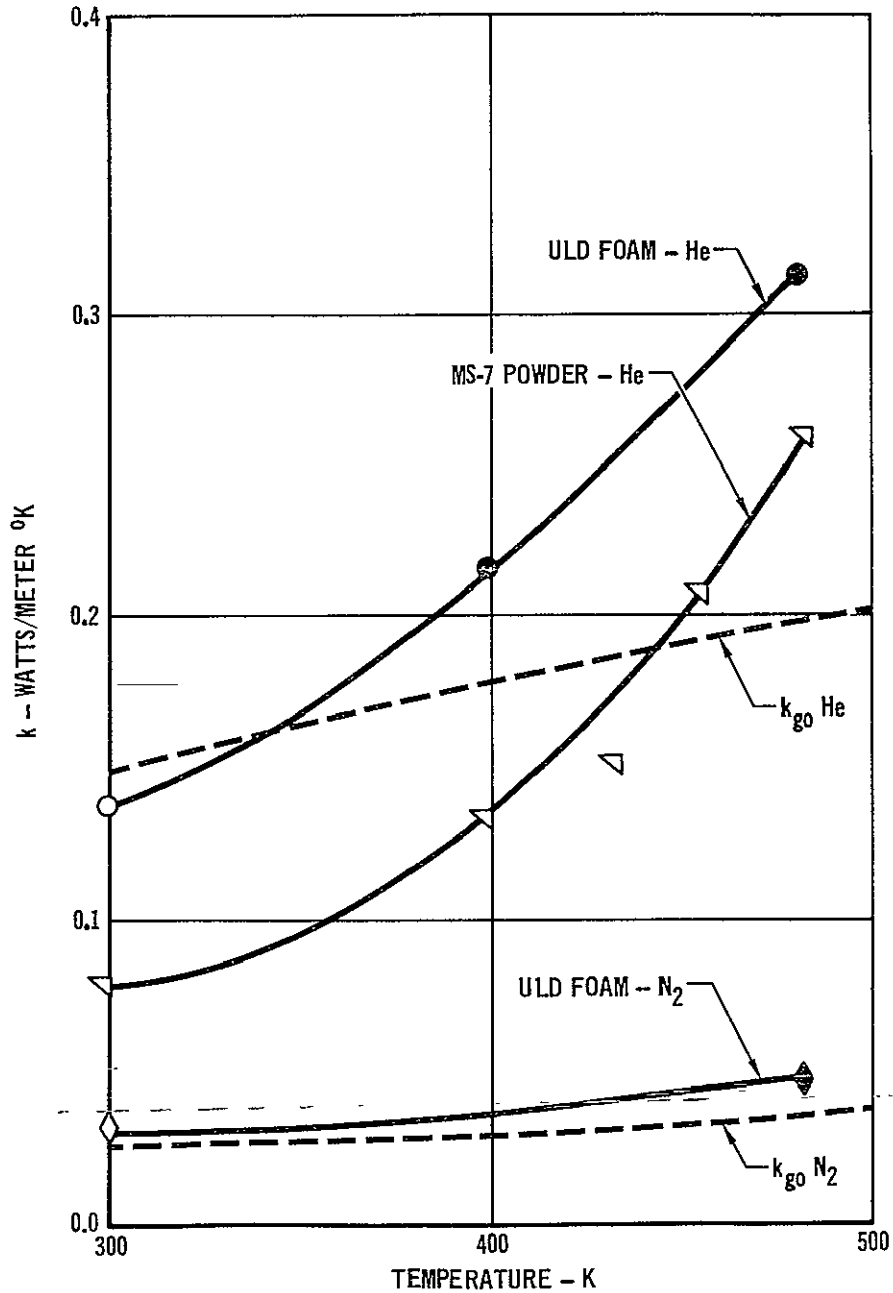


FIGURE 33 LIMITING CASES OF HEAT TRANSFER



In summary, the values of the thermal conductivity data measured in this program could not be completely explained. Additional tests at one atmosphere pressure were run on the ULD filled specimen to try to improve our understanding of what was happening. The results are presented in Figure 34. For the helium environment, the sharp rise in conductivity with temperature was in evidence, but in a nitrogen environment the trend was greatly reduced. Again, the magnitude of the differences between the two gases cannot be fully explained, but it does reaffirm that radiation heat transfer is not a predominant term.

FIGURE 34 ULD CONDUCTIVITY AT ONE ATMOSPHERE PRESSURE



10.0 ADDITIONAL TESTING

Because the data could not be fully explained, we felt that some systematic error might have been introduced by the test specimens or test setup. Thus, we redesigned and retested a MS-7 powder mixture at an independent laboratory. A schematic of the redesigned specimen is shown in Figure 35. Both facesheets were made from stainless steel to minimize the warping problem and to allow the thermocouples to be mounted directly into the facesheets. The H/C was slotted on one side to allow all the individual cores to be directly vented. This improved the venting characteristics by allowing all of the core to be vented directly. Two filters, each made up of two layers of phenolic fiberglass cloth, were bonded around the edge of the specimens to retain the powder. The powder mixture was mixed and tapped into the specimen for eight hours in an identical fashion as the original specimen. We obtained a powder density of 120 kg/m^2 (7.5 lbm/ft^3) which was very close to the density of the original specimen. MDAC selected Southern Research Institute (SRI) in Birmingham, Alabama to test the new specimens. A complete description of the SRI test is presented in Appendix C. Each test point was repeated at least once. The results of these tests are shown in Figure 36 along with an estimation of the conductivity that could be expected for the empty core.

FIGURE 35 REDESIGNED SPECIMEN CONFIGURATION

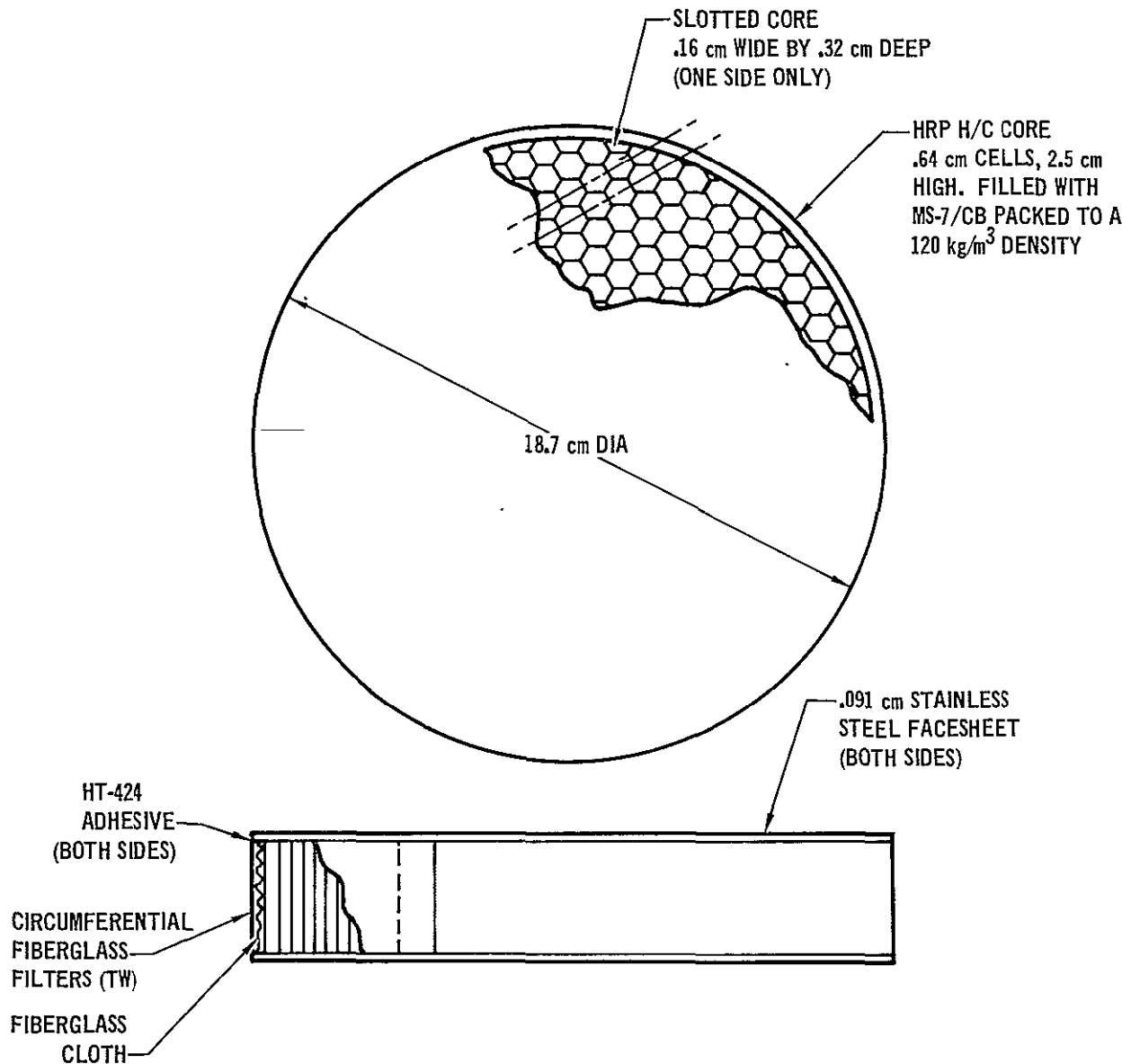
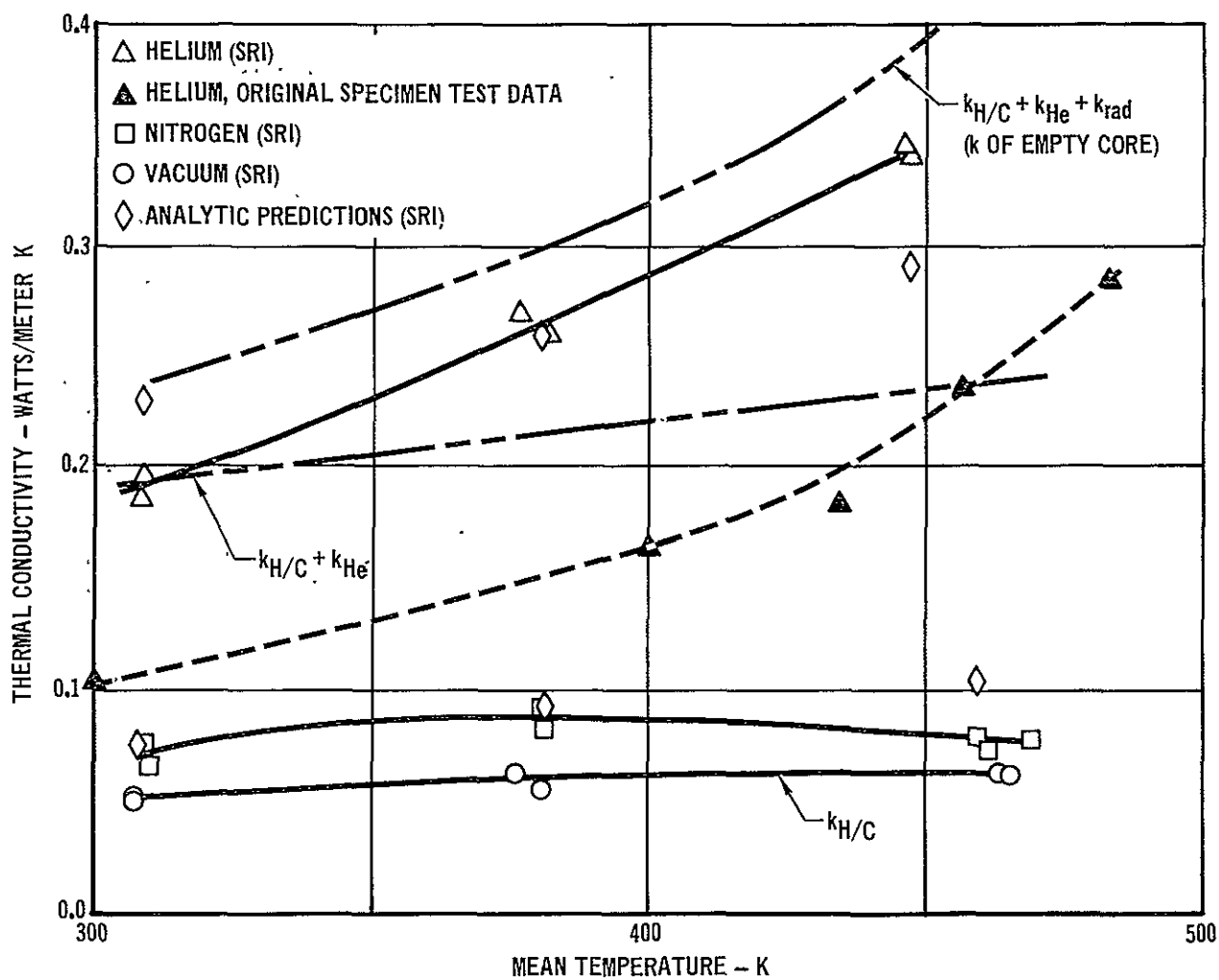


FIGURE 36 REDESIGNED SPECIMEN TEST DATA - ONE ATMOSPHERE PRESSURE



11.0 DISCUSSION OF THE RESULTS OF ADDITIONAL TESTING

The redesigned specimens yielded results that were substantially higher than the original test data in helium. Although the original specimens had some warpage present, it would not contribute to this magnitude of a difference. Although small differences might occur due to different set up procedures at the different laboratories, large differences would not be expected since both tests were run by the procedures outlined in ASTM C-177. The venting design of the two specimens, though, were different. The specimens designed and built by MDAC-E for testing at SRI had all individual cores vented to the ambient through the slots cut across the top of the cores. The original specimens had only about 10% of the cores vented directly to the ambient, with the venting of the remaining cores left to gas diffusions through the thin H/C walls. It seems quite probable that there was inadequate venting in some of the cores resulting in a mixture of N₂ and He gas in the specimens for the test in the helium environment. This gas mix would result in a lower measured thermal conductivity in the original specimens which is what was observed. The sharper rise with temperature of the original data could be partially due to increasing the concentration of helium in the cores due to the higher temperatures and longer duration of exposure to the ambient helium environment. The data measured using the redesigned specimen are believed to be more representative data.

Unfortunately, this leaves an even larger problem to be resolved: why is the conductivity so high? As shown in Figure 36, the results in helium indicate that the conductivity of the filler in He is actually higher than the conductivity of the gas. To explain the data analytically, Dr. McDonald at SRI used the series-parallel formulations of Equation (3) to derive the analytic values shown in Figure 36. (See Appendix C for the details). His basic assumption, though, was that the gas trapped between solid particles had the conductivity of the unrestrained gas, i.e., $k_{ge} = k_{go}$. Since this did agree with the data within 20%, we must conclude that the powder is ineffective in reducing the effective conductivity of the helium gas at one atmosphere pressure. The analytic predictions do not completely explain the steep slope of the helium data or the tailing off of the nitrogen data. Because of the care that was taken in running the tests and the three repeated points, it is believed that the leveling off of the high temperature nitrogen data represents a real trend rather than scatter in the data. A somewhat similar phenomenon was observed in the second set of ULD testing as shown in Figure 34. It is interesting to note that the leveling off of the data might be indicative of the powder working for the nitrogen gas (see k_{ge} on Figure 30). Although the data was higher than expected, Figure 36 shows that the net conductivity is slightly below what would be expected for an empty core.

12.0 CONCLUSIONS AND RECOMMENDATIONS

The thermal conductivity testing of the candidate insulation concepts yielded results that were much higher than expected. Independent testing of a redesigned test specimen showed a further increase in the thermal conductivities when compared to the original specimens with the same filler material. It is believed that the original data in helium were not correct due to N_2 gas not being completely vented from the core before filling with He. The retests showed that the powders are not effective in reducing the thermal conductivity of the gas at one atmosphere pressure. No additional tests were run at pressures other than one atmosphere. In both tests the helium environment induced a larger increase in thermal conductivity than could be explained, while the nitrogen data leveled off with increasing temperature. None of the classical modes of heat transfer as combined in the analysis can completely explain the trends apparent in the data. Since the combined heat transfer mechanism is not well understood, the test data cannot be extended to other gases, such as hydrogen which is the major constituent of the atmospheres of the outer planets.

In general, simple theory cannot be used to predict insulation performance in the typical outer planet atmospheres. At pressures above one atmosphere, the powder fillers do not reduce the effective thermal conductivity of helium gas, but the radiation contribution is blocked. Although the foam was not retested in the redesigned specimen, the qualitative results of the original tests indicated higher conductivities than in the powders.

The results of the structural bond strength test indicated that neither the powders or the foam are acceptable for use in the OPP unless other processes can be found to insure bond strength integrity. The powders were difficult to work with, and even if an acceptable bonding process could be found, packing the powder mixture in the conical H/C of the OPP would present a burdensome fabrication problem. The foam was easier to work with. Alternate processing methods, such as curing the foam before bonding, or the use of alternate foams such as epoxy base, might allow acceptable bond strengths. Before any future thermal tests are performed, it is recommended that candidate insulative fillers and processes be tested to insure acceptable bonding properties.

The test results show only a marginal improvement in the H/C thermal insulation performance for a powder filled core compared to an unfilled core, and uncovered potential structural and manufacturing difficulties. For these reasons, it is recommended that an empty forward H/C core be adopted as the baseline design for the OPP, and that the empty core be tested under the full range of conditions that might be encountered during entry and descent into the outer planet atmospheres to obtain accurate data for the conduction/convection/radiation interchanges within the empty core. If the radiation and/or convection rates prove to be excessive, alternate filler materials, e.g., foams, RSI material, or Min-K, might be acceptable if processes can be formulated to insure bond strength integrity. Since the differences resulting from the different gases could not be fully explained, it is recommended that any future thermal conductivity test be conducted in a hydrogen/helium environment representative of the atmospheres of the outer planets.

REFERENCES

1. "Saturn/Uranus Atmospheric Entry Probe, Final Report, Part II, Technical Discussion", MDC Report E0870, 18 July 1973.
2. "Cabot Carbon Blacks", Cabot Corporation Brochure.
3. "Cab-O-Sil", Cgew-7, Cabot Corporation Brochure.
4. "Thermal Conductivity of Packed Beds", Schotte, W., A.I.Ch.E Journal, March 1960.
5. "Non-Evacuated Cryogenic Thermal Insulation Sutides", Johnson, C. L. and Hollweger, D. J., ML-TDR-64-260, September 1964.
6. "Heat Transfer by Gas Conduction and Radiation in Fibrous Insulations", Verschoor, J. D. and Greebler, P., Transactions of the ASME, August 1952.
7. "Thermal Conductivity Measurements of Porous Materials in Several Gaseous Environments at Subatmospheric Pressures", Keshock, E. G., AIAA Paper No. 73-95, January 1973.
8. "High Temperature Insulation Materials for Reradiative Thermal Protection Systems", Hughes, T. A., NASA CR 123945 (Report MDC E066), July 1972.
9. "Heat Transfer by Radiation and Conduction in Evacuated Powders", Wechsler, A. E., Proceedings of the Sixth Conference on thermal Conductivity, Dayton, Ohio, October 19-21, 1966.
10. "Heat Transfer Mechanisms in Evacuated Powder Insulations", Glaser, P. E., 1961 International Heat Transfer Conference, Paper No. 100, Vol IV, 1961.
11. "Kinetic Theory of Gases", Kennard, E. H., McGraw-Hill Book Co., 1938.
12. "The Properties of Gases and Liquids", Redi, R. C., Sherwood, T. K., McGraw-Hill Book Co., 1966.
13. "Transport Phenomena", Bird, R. B., Steward, W. E., and Lightfoot, E. N., John Wiley & Sons, 1962.
14. "Natural Convection in Enclosed Porous Media with Rectangular Boundaries", B. K. C. Chan, C. M. Ivey, J. M. Barry, Journal of Heat Transfer, February, 1970, pp 21-27.
15. "Natural Convection in a Sloping Porous Layer", S. A. Bories, M. A. Combarous, J. Fluid Mechanics, (1973), Vol. 57, Part 1, pp 63-79.
16. "Criterion for the Onset of Convective Flow in a Fluid in a Porous Medium", Y. Kalto, T. Masuoka, International Journal of Heat and Mass Transfer, (1967), Vol. 10, pp 297-309.
17. "Steady Free Convection in a Porous Medium Heated from Belw", J. W. Elder, Journal of Fluid Mechanics (1967), Vol. 27, Part 1, pp 29-48.
18. "Effect of Side Walls on Natural Convection Between Horizontal Plates Heated from Below", I. Catton, D. K. Edwards, Journal of Heat Transfer, November 1967, pp 295-299.
19. "Convection in a Closed Rectangular Region: The Onset of Motion", I. Catton, Transactions of the ASME, February 1970, pp 186-187.
20. "Natural Convection in Horizontal Thin-Walled Honeycomb Panels", K. G. T. Hollands, ASME-72-HT-60.
21. "Convection in Boxes Experiments", K. Stork, U. Muller, Journal of Fluid Mechanics (1972), Vol. 54, Part 4, pp 599-611.
22. U. S. Department of Commerce National Bureau of Standards, File No. 81-30, February 20, 1958.
23. "Mechanical Properties of Hexcell Honeycomb Materials", TSB-120, pp 19, Hexcell Aerospace Corporation, August 1971.
24. "Insulation Testing Under Venus Environmental Conditions", D. P. Crowley and P. Livine, AIAA 72-368, April 1972.
25. "Thermal Conductivity of Porous Media in Unconsolidated Sands", Journal of Applied Physics, Vol. 32, No. 9, September 1961.

ACKNOWLEDGEMENTS

The writers are grateful to Messrs. Thomas Hughes and Eugene Rusert for their expertise in the selection and fabrication of the test specimens, to Mr. Vernon Holmes who conducted the thermal conductivity tests, to Mr. James Smittkamp for his help in the structural testing, and to Dr. John McDonald of Southern Research Institute for his effort in the additional testing. The suggestions and patience afforded by Mr. John Givens (NASA/ARC Technical Monitor) and Dr. Craig McCreight (NASA/ARC) are appreciated.

APPENDIX A

PROPERTIES OF THE GASES AND FILLERS

A. GAS PROPERTIES

 THERMAL CONDUCTIVITY AT 1 ATM PRESSURE -

 REF: "ANALYSIS OF HEAT AND MASS TRANSFER," E. R. G. ECKERT AND R. M. DRAKE

HELIUM		NITROGEN	
T (K)	k_{go} WATTS/METER K	T (K)	k_{go} WATTS/METER K
200	0.1177	200	0.01824
255	0.1357	300	0.02620
366	0.1691	400	0.03335
477	0.1970	500	0.03984
589	0.2250		

DIAMETER OF MOLECULE

d cm

REF: "KINETIC THEORY OF GASES," E. H. KENNARD

CONSTANTS

$R = .08205$ ATM-LITERS/MOLE - K

$N = 6.025 \times 10^{23}$ MOLECULES/MOLE

GAS	d cm
He	2.18×10^{-8}
N ₂	3.75×10^{-8}

B. POWDER PROPERTIES

TYPE	AVERAGE PARTICLE DIAMETER \AA	DENSITY OF BULK MATERIAL kg/m^3 (lbm/ft ³)	DENSITY OF SOLID MATERIAL kg/m^3 (LBM/ft ³)	SURFACE AREA m^2/gm
CARBON BLACK MONARCH 1100	140	240 (15)	1800.3 (112.4)	240
SILICA POWDER CAB-O-SIL EH-5	70	36.8 (2.3)	2199.1 (137.3)	390
SILICA POWDER CAB-O-SIL MS-7	120	72.1 (4.5)	2199.1 (137.3)	200

REF: CABOT CORP., 125 HIGH STREET, BOSTON, MASS. 02110

C. HONEYCOMB CORE PROPERTIES

MATERIAL: PLASTIC LAMINATE CTA-A CTA-A
 PHENOLIC, 28.3% - 181 GLASS

CELL SIZE: .64 cm (.25 IN.)

CELL HEIGHT: 2.54 cm (1.00 IN.)

DENSITY: 136 kg/m³ (8.5 lbm/ft³)

DENSITY OF SOLID MATERIAL: 1762 kg/m³ (110 lbm/ft³)

SOLID VOLUME FRACTION: .076

D. SPECIMEN WEIGHTS AND THICKNESSES

SPECIMEN NUMBER	HONEY COMB (gm)	ALUM* PLATE (gm)	ADHESIVE ALUM SIDE (gm)	ADHESIVE PHENOLIC SIDE (gm)	PHENOLIC* PLATE (gm)	FILLER (gm)	WEIGHT* AFTER FINAL BONDING (gm)
1	109.69	149.10	22.28	20.91	69.83		371.8
2	109.15	148.57	22.69	22.32	71.10		373.9
3	108.99	149.13	21.68	26.20	85.24	61.1	452.3
4	109.35	147.23	21.78	27.22	86.00		
5	109.78	148.52	21.54	26.43	85.31	56.3	447.8
6	109.05	148.32	21.40	26.41	85.45	85.2	475.8
7	109.49	148.05	21.98	26.82	86.10	83.8	476.3
8	112.45	147.79	22.00	26.80	86.75	105.1	501.0
9	110.04	149.01	21.20	26.20	85.50	110.6	502.5

AVERAGE VOLUME OF THE CORE = 680 ml

SPECIMEN THICKNESS

	ALUM* FACE PLATE (cm)	ADHESIVE ALUM SIDE (cm)	CORE (cm)	PHENOLIC* (cm)	ADHESIVE PHENOLIC SIDE (cm)
1	0.165	0.041	2.553	0.130	0.041
2	0.163	0.043	2.535	0.132	0.041
3	0.165	0.041	2.545	0.132	0.041
4	0.163	0.041	2.543	0.130	0.041
5	0.165	0.041	2.545	0.132	0.041
6	0.165	0.051	2.543	0.132	0.041
7	0.163	0.041	2.537	0.130	0.041
8	0.163	0.041	2.540	0.132	0.041
9	0.165	0.041	2.545	0.132	0.041

*PRIOR TO SANDING OF EXTERNAL FACEPLATES

E. PROPERTIES OF FILLERS IN TEST SPECIMENS

PROPERTIES OF A 50-50 MIXTURE BY WEIGHT OF CARBON BLACK AND Cab-O-Sil

MIXTURE	VOLUME Cab-O-Sil TOTAL SOLID VOLUME	AVERAGE DENSITY OF SOLID MATERIAL kg/m ³ (lbm/ft ³)	AVERAGE PARTICLE DIA. Å
CB/EH-5	.867	1980 (123.6)	79
CB/MS-7	.769	1980 (123.6)	125

FILLER	SPECIMEN NO.	AVERAGE FILLER DENSITY kg/m ³ (lbm/ft ³)	f SOLID VOLUME FRACTION
CB/EH-5	3,5	85.7 (5.35)	.0485
CB/MS-7	6,7	124.1 (87.75)	.0647
ULD	8,9	161.8 (101.1)	NA

REPRODUCIBILITY OF THE
ORIGINAL PAGE IS POOR

APPENDIX B

THERMAL CONDUCTIVITY TEST APPARATUS

The thermal conductivity of the honeycomb sandwich panels was measured in a guarded hot plate type calorimeter following the general procedures outlined in ASTM C-177. The guarded hot plate calorimeter used a 10.2 cm (4 in.) diameter flat central heater guarded by a flat 10.7 cm (4.2 in.) ID, 20.3 cm (8 in.) OD guard heater as shown in Figure B-1. The central/guard heater was sandwiched between two identical test specimens which were sandwiched between water cooled cold plates on the outside. The simple cold plate consisted of a flat copper plate with a cooling coil spirally attached. For the higher temperature runs cold plate heaters with water-cooled cold plates on the outside surfaces were used. As shown schematically in Figure B-2, the heaters attached to the inside surface of the cold plates permitted control of the specimens' mean temperature and total temperature differential across the sample. A differential thermocouple averaged the temperature at several points around the central guard heater interface. The differential thermocouple was attached to a temperature controller to maintain the guard within 1°C of the temperature of the control heater. Radial heat flow from the central test section was reduced to a negligible value with this system. Thermocouples were installed on each side of the test specimens. The thermocouples were physically bonded to the specimens in the center. Other thermocouples were spaced radially from the center to measure temperature distributions across the specimens.

FIGURE B-1 GUARDED HOT PLATE

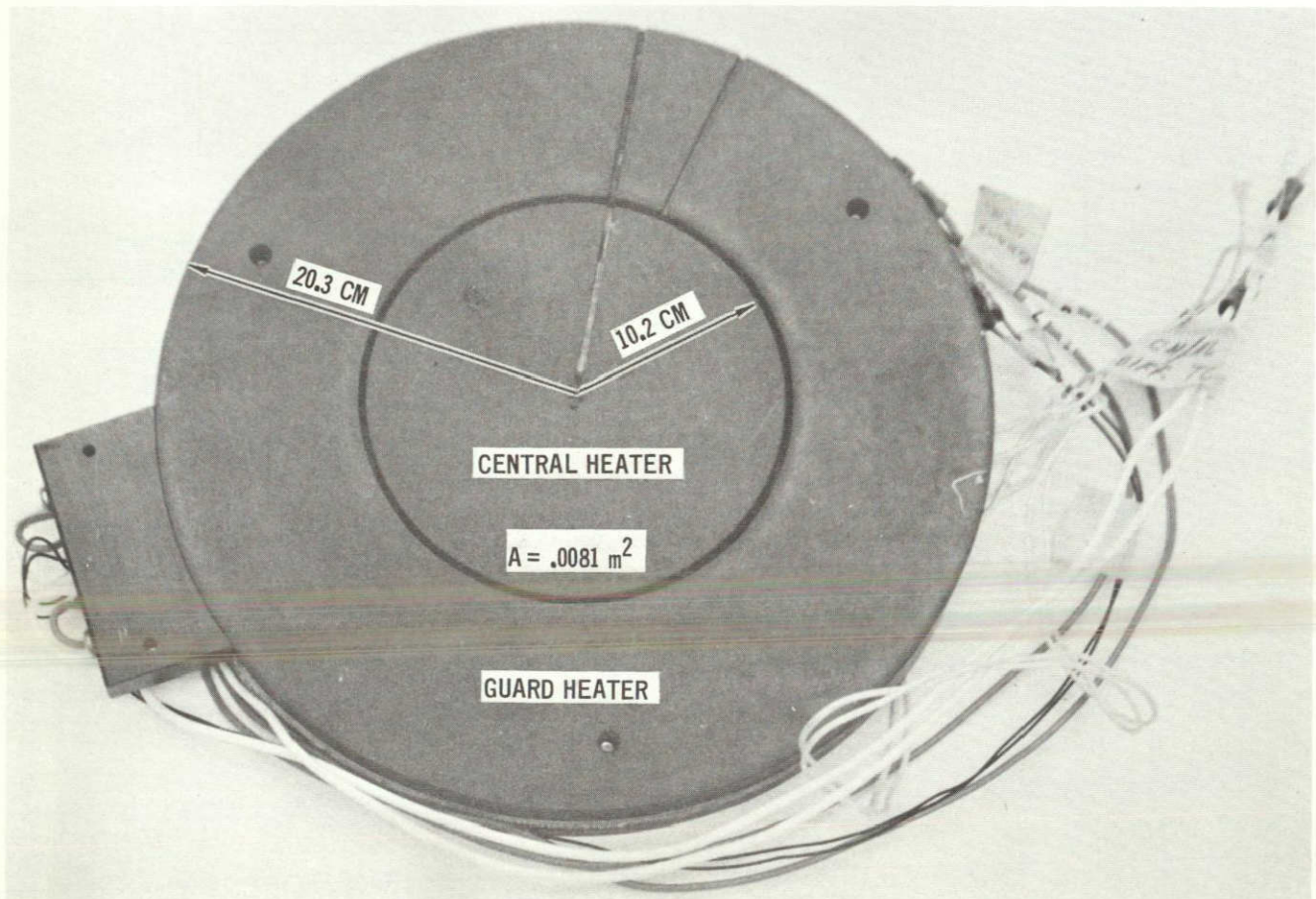
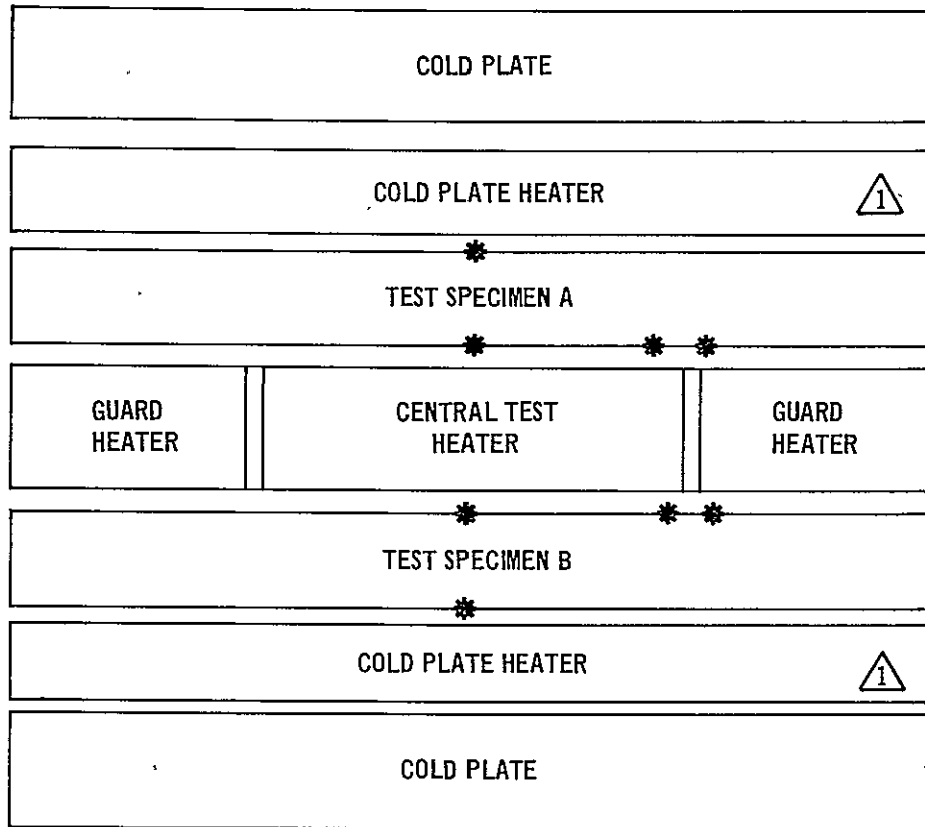


FIGURE B-2 SCHEMATIC OF THE SPECIMEN INSTALLATION IN THE GUARDED HOT PLATE CALORIMETER



* THERMOCOUPLES

△ 1 USED ONLY FOR SPECIMEN MEAN TEMPERATURES ABOVE 200°F

To establish each desired test mean temperature, the power was adjusted to the central heater several times and then left for several hours to reach a steady state temperature distributions through the composite test stack. After temperature equilibrium had been established temperatures were measured using a Leeds-Northrup 8686 potentiometer. An ammeter and voltmeter were used to measure the current supplied to the central heater and the voltage drop across the heater itself.

APPENDIX C

Southern Research Institute



2000 NINTH AVENUE SOUTH
BIRMINGHAM, ALABAMA 35205
TELEPHONE 205-323-6592

December 5, 1975

Mr. Mike Grote
McDonnell Douglas Corporation
Post Office Box 516
St. Louis, Missouri 63116

Dear Mr. Grote:

INTRODUCTION

This is a final report to McDonnell Douglas Corporation, for work performed under P. O. No. Y5E154. This program involved thermal conductivity evaluations on a powder filled fiberglass honeycomb sandwiched with stainless steel face plates. Evaluations were performed in vacuum, nitrogen, and helium environments at three temperature levels, 95°F, 225°F, and 375°F, +5°F.

MATERIAL DESCRIPTION

Two specimens were supplied by McDonnell Douglas Corporation. Each specimen consisted of a fiberglass honeycomb structure sandwiched between two stainless steel face plates. The honeycomb was packed with a filler material consisting of a 50-50 mixture of carbon black and silica powder (CAB-O-SIL MS-7) packed to a density of about 7.8 lb/ft³.

The specimens received were about one inch thick and 7.38 inches in diameter, a schematic drawing of the structure is shown in Figure 1. The stainless steel face plates were 0.036 inches thick machined flat to within 0.005 inches per foot on both sides. The honeycomb core made ~~of phenolic fiberglass consisted of one-fourth inch hexagonal cells one~~ inch high. The phenolic fiberglass cell walls occupied about 7.6 percent of the total area. The honeycomb (H/C) core was slotted to allow diffusion of the particular gas environment throughout the specimen, and secured by bonding fiberglass cloth around the H/C core at the overlaps. Each individual cell was filled with a powder consisting of a 50-50 mixture by weight of carbon black and CAB-O-SIL.

The mixture had a void volume fraction of 0.9353 (properties of specimen components supplied by McDonnell Douglas Corporation).

The thermal conductivity measurements were made in the "axial" direction, defined as being perpendicular to the stainless steel face plates.

APPARATUS AND PROCEDURE

Thermal Conductivity

The ASTM C-177 guarded hot plate was employed to determine the thermal conductivity of the honeycomb structure at three temperature levels, 95°F, 225°F, and 375°F in three environments, vacuum, nitrogen gas, and helium gas.

Guarded Hot Plate Apparatus. A complete description of the ASTM C-177 guarded hot plate apparatus is included in Appendix A, and a schematic of the build-up is shown in Figure 3. For these evaluations the middle size apparatus with the 7-3/8 inch heater plate was employed. Due to the nature of these particular specimens, the evaluations required the following exceptions to the described procedures:

1. The two specimens were solid, that is, not split into a central and guard ring.
2. Temperatures on all runs were measured at the surface of each specimen with thermocouples inserted into small pin holes and secured by pinging. The thermocouples were beaded 0.005 inch diameter chromel/alumel bare wires.
3. The bare thermocouple wires were insulated from the specimen surface by painting a 3/4 inch wide strip with a non-electrically conductive paint, placing a strip of teflon tape on top of the paint, laying the bare thermocouple wires on the tape, and placing another strip of teflon tape on top of the wires completely insulating the wires except for specimen contact. Care was taken to insure the wires touched only at the thermocouple junction located at the central region of the specimen.
4. McDonnell Douglas required a temperature drop of 50°F \pm 5°F across the specimens at each temperature level. This was maintained at each temperature except at a specimen mean temperature of about 375°F in the three environments. At this temperature the ΔT across the specimen was approximately 100°F in environments of nitrogen and helium gas and 85°F in vacuum. Due to the low conductivity of the specimens, it was necessary to place in series with each specimen a one inch thick piece of low thermal conductivity insulation material (Min K) to maintain the 100°F ΔT across each specimen.

Actual ΔT 's for each run are plotted versus power to the central heater area in Figures 4, 5, and 6.

DATA AND RESULTS

Thermal Conductivity

Model Analysis. To provide more meaningful input to the computation of heat transfer through the powder filled H/C structure, a thermal model is presented which allows the determination of the effective thermal conductivity of the system given the conductivities and volume fractions of its components. The model was also developed to substantiate the measured experimental values. This was necessary since the discrepancy between data taken in vacuum and helium environments was greater than that obtained by adding (in the proper proportion) the thermal conductivity of helium gas to the vacuum data.

The effective thermal conductivity, sometimes called the stagnant conductivity, of unconsolidated particles containing a nonflowing fluid is a function of the thermal conductivities of the solid and fluid phases, the void fraction, and if radiation is important, the emissivity, mean temperature, and diameter of the solid particles.

The contribution due to radiation and convection heat transfer has been neglected in the proposed model. Radiation was not included since the maximum temperature is only 375°F and at this temperature the radiative heat transfer in a gaseous fluid is negligible. Convection heat transfer was not included for two reasons, first it was decided the stagnant gas would not transport sufficient energy for convection to occur. Second, for natural convection the heat transfer coefficient is proportional to the Rayleigh number raised to a power, usually to the 1/4 or 1/3 power depending on whether the regime is laminar or turbulent convection. The Rayleigh number is a product of the Prandtl and Grashof numbers. For free or natural convection equality of the Grashof number establishes dynamic similarity. The Grashof number represents the ratio of buoyant to viscous forces, and the buoyant effect is the driving force in free convection. For this analysis the temperature of the gas environment was taken as the specimen mean temperature and any gas density variation over the one inch specimen thickness was considered negligible, hence free convection was not considered.

Figure 2 illustrates the thermal model devised to simulate heat flow through the specimen. Basically, the structure of the model consists of the powder and gas in parallel with the phenolic fiberglass cell walls and these two in series with the stainless steel face plates.

To analyze the model, first the thermal conductivity of the powder filled with a foreign gas will be determined, then the addition of the phenolic fiberglass in parallel, and finally the face plates in series.

The powder filler consists of particles in contact with each other surrounded by a stagnant fluid. Heat transfer is assumed to occur in the vertical direction by the following mechanisms:

1. Heat transfer through the gas in the void space by conduction.
2. Heat transfer through particles in close or point contact with each other to form continuously conducting paths.
3. Heat transfer through particle and gas in series.

As mentioned, mechanism three considers the solid particles and gas in series and the model requires mechanisms 1, 2, and 3 to be in parallel, this is consistent with previous investigators. The model is thus a combination of the series and parallel distributions. For the gas-filled powder, it follows from Figure 2, that k , the effective thermal conductivity is given by:

$$k = \frac{a k_s k_f}{k_s (1-d) + d k_f} + b k_s + c k_f \quad (1)$$

where k_s is the thermal conductivity of the solid material from which the powder is derived, and k_f the thermal conductivity of the gas filling the pore space. The parameters a , b , c , and d must be calculated based on the geometry of the model, known void fraction of the powder, the conductivity of the powder measured in vacuum, and an empirical relationship used by Woodside and Messmer¹ to determine c . Considering unit area for the powder filled gas, the following relation applies:

$$a + b + c = 1 \quad (2)$$

This relation follows from (1) by applying the condition that when $k_s = k_f$, k must also equal k_f . It is also apparent that:

$$ad + b = 1 - \phi \quad (3)$$

¹Woodside, W., and Messmer, J.H., "Thermal Conductivity of Porous Media. I. Unconsolidated Sands", Journal of Applied Physics, Vol. 32, Number 9, September, 1961.

where ϕ = void volume fraction of powder. This relation states the volume occupied by the solid is equal to the solid volume fraction.

This gives two equations for determining the parameters. Another relationship is evident from (1) that when $k_f = 0$, $k = b k_s$, this represents the straight through solid conduction. The condition $k_f = 0$ may be closely approximated by evacuating the specimens, and the value of b was determined by:

$$b = k_{\text{vac}}/k_s \quad (4)$$

In order to determine the parameter b at, for instance, a specimen mean temperature of 350°F, the thermal conductivity of the gas filled powder in vacuum was calculated using the thermal model and the specimen measured value in vacuum, which is 0.41 Btu in./hr ft²°F. This gave a value of 0.0031 for b which falls within the range of values obtained by Woodside and Messmer.¹

For unconsolidated porous media, many investigators have employed a similar model for particles having void fractions less than 0.6, and have used an electrical relation for the parameter c . Comments by Woodside and Messmer¹ indicate this relation gives low conductivity values and suggested the following empirical equation which was used in this model and with success in the model of Woodside and Messmer¹:

$$c = \phi - 0.03 \quad (5)$$

Using the known value for ϕ (0.9353), c was determined to be 0.9053, and remains constant at each temperature level. With b and c known, a and d can be determined from the constraint equations (2) and (3). At a specimen mean temperature of 375°F the values of the four parameters were determined to be:

$$\begin{aligned} a &= 0.0916 \\ b &= 0.0031 \\ c &= 0.9053 \\ d &= 0.6725 \end{aligned} \quad (6)$$

The powder is a 50-50 mixture of carbon black ($k \approx 48$ Btu in./hr ft²°F) and silica ($k \approx 9.6$ Btu in./hr ft²°F). Therefore, k_s was determined to be 28.8 Btu in./hr ft²°F.

The thermal conductivity, k_f , of the gas occupying the voids in the powder must be determined. For a gas in the free state, the distance an average molecule travels before collision (the mean free path) is a function of the number of other molecules present. In a confining structure the mean free path may be increased by decreasing the gas pressure until the mean free path is determined by molecular collision with the containing boundaries. Continually reducing the pressure reduces the gas density without further reduction in the mean free path which would result in a lower gas thermal conductivity.

Mr. Grote
McDonnell Douglas
Page 6
December 5, 1975

Southern Research Institute

Many investigators have simulated the same effect by reducing the distance between molecular boundaries rather than reducing the gas pressure. This has been achieved by using fine powders, foams, and fibrous materials.

For the thermal model presented here, it was decided that the thermal conductivity of the gas environment should be used in totality. Reasons for this are three fold, first the void fraction of the powder is large (0.9353), second the individual particles of carbon black are not spherical, and actually resemble popcorn under a microscope, and thirdly the particles in commercial powders tend to form agglomerates. For these reasons at each temperature level, k_f was taken to be the thermal conductivity of the gas environment at one atmosphere pressure.

Applying the above parameters, the effective thermal conductivity of the gas-filled porous powder is determined from (1). The gas-filled powder is in parallel heat transfer with the phenolic fiberglass cell walls and the parallel conductivity of these two constituents become:

$$k_{\text{parallel}} = (1-f)k_p + f k_{fg} \quad (7)$$

where f is the solid volume fraction of the H/C cells, and k_{fg} is the thermal conductivity of the phenolic fiberglass. k_{fg} was varied from about 3 Btu in./hr ft²°F at RT to about 4 Btu in./hr ft²°F at 375°F. The solid volume fraction of the H/C was given as 0.076 by MDAC.

The final calculation considers the parallel component from (7) in series with the two stainless steel face plates. Referring to the thermal model, the total effective thermal conductivity of the specimen is determined by the three constituents in series,

$$\frac{1}{k_t} = \frac{1}{k_{ss} \left(\frac{1}{0.036} \right)} + \frac{1}{k_{\text{par}} \left(\frac{1}{0.928} \right)} + \frac{1}{k_{ss} \left(\frac{1}{0.036} \right)} \quad (8)$$

where k_{ss} = thermal conductivity of 316 stainless steel at one atmosphere pressure.

Applying equation (8) for a helium environment at one atmosphere at a specimen mean temperature of 225°F k_t was calculated to be 1.81 Btu in./hr ft²°F compared to the measured value of 1.80 Btu in./hr ft²°F. Table 1 tabulates analytical and experimental values at each test condition.

Mr. Grote
McDonnell Douglas
Page 7
December 5, 1975

Southern Research Institute

In both helium and nitrogen environments the analytical values are higher at a specimen temperature of 95°F, and in helium gas at 345°F the analytical value is lower than experimental. In nitrogen gas at 367°F the analytical value is somewhat higher than the measured value, 0.718 Btu in./hr ft²°F compared to 0.548 Btu in./hr ft²°F. In nitrogen, one would suspect the measured value to be low, since the character of the curve and analytical values indicate the total conductivity of the specimen should increase slightly with increasing temperature.

Figures 7, 8, and 9 illustrate the thermal conductivity of the H/C specimen in vacuum, nitrogen gas, and helium gas over the temperature range, and are tabulated in Tables 2 thru 7. Superimposed on the curves in helium and nitrogen gas environments are the analytically calculated points:

Figure 10 is a comparison of the data measured in the three environments. The vacuum data indicates the specimen thermal conductivity increases slightly from 0.361 Btu in./hr ft²°F at 93°F to a value of 0.439 Btu in./hr ft²°F at 378°F.

To check the ASTM C-177 apparatus, a plexiglass standard was run in vacuum, helium gas, and nitrogen gas at a temperature of about 90°F and as expected, there were no significant increase between the data in the different environments, and the magnitude of the thermal conductivity was within the uncertainty of the apparatus, ±5 percent. The thermal conductivity of plexiglass was measured to be about 1.25 Btu in./hr ft²°F at 90°F.

CONCLUSIONS

The thermal conductivity of a powder filled H/C structure was determined in vacuum, helium gas, and nitrogen gas. A thermal model was analyzed to simulate heat transfer through the specimen. Other investigators have assumed a similar model when simulating heat transfer through a porous media filled with a foreign gas. The only discrepancy between the models, is the value used for the thermal conductivity of the gas filling the voids. For reasons discussed earlier, the thermal conductivity of the gas phase at each temperature was taken as the value for the gas at one atmosphere, and not calculated based on the mean free path of the gas and particle diameter (~100Å). Applying this condition, the analytical value compares very well with measured values at the mid temperature point, 225°F and deviates slightly at the two end temperatures. The model does account for the increase in the thermal conductivity when testing in vacuum and helium or nitrogen gas. This increase is larger than simply adding the value for helium or nitrogen gas to the vacuum data.

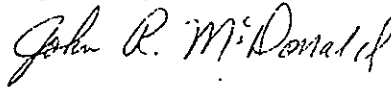
Mr. Grote
McDonnell Douglas
Page 8
December 5, 1975

Southern Research Institute

ACKNOWLEDGMENTS

The thermal conductivity evaluations and model analysis performed under this program were coordinated by Dr. J. R. McDonald, Head, Applied Thermal Section. The experimental evaluations were performed by Mr. William Reid, Research Technician, Applied Thermal Section under the supervisor of Mr. Andre' P. Wooten, Supervisor, Applied Thermal Section. Mr. C. D. Pears offered valuable input to simulating the heat transfer through the powder filled H/C and aided in the model analysis.

Very truly yours,



J. R. McDonald, Head
Applied Thermal Section

Approved:



C. D. Pears, Director
Mechanical Engineering Research
Department

SORI-EAS-75-615-3567-I-F

JRM:dcb

FIGURE 1 SPECIMEN CONFIGURATION

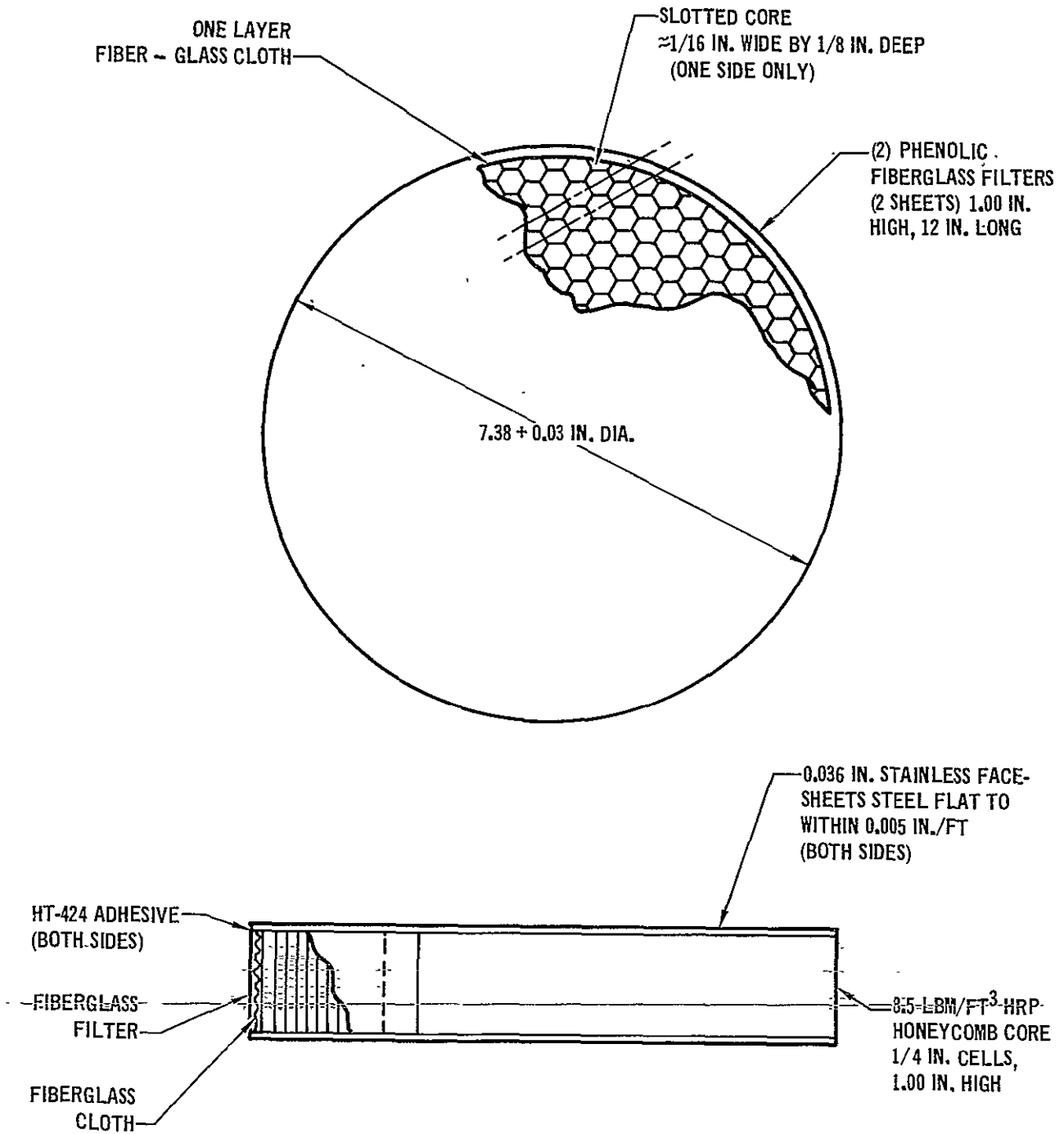


FIGURE 2 THERMAL MODEL

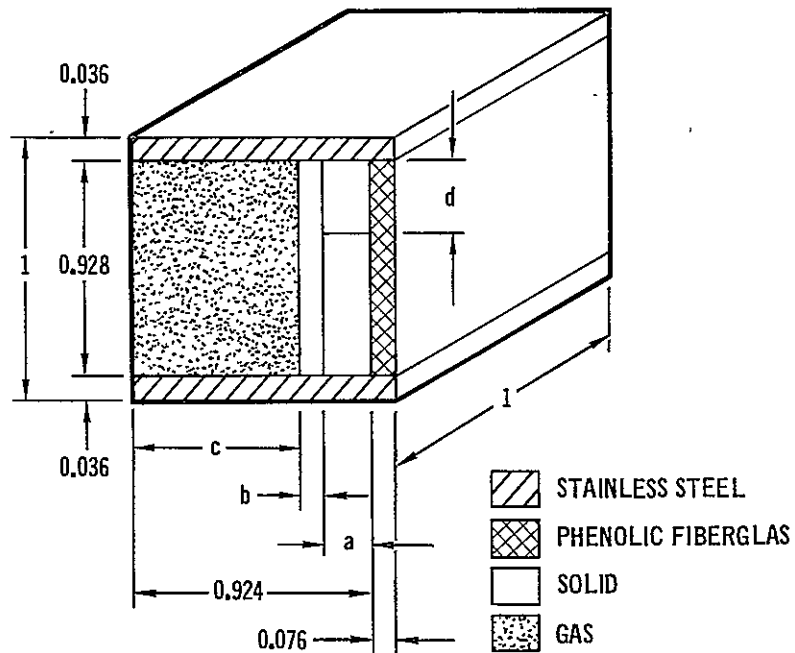


FIGURE 3. SPECIMENS BUILD-UP IN ASTM C-177 APPARATUS

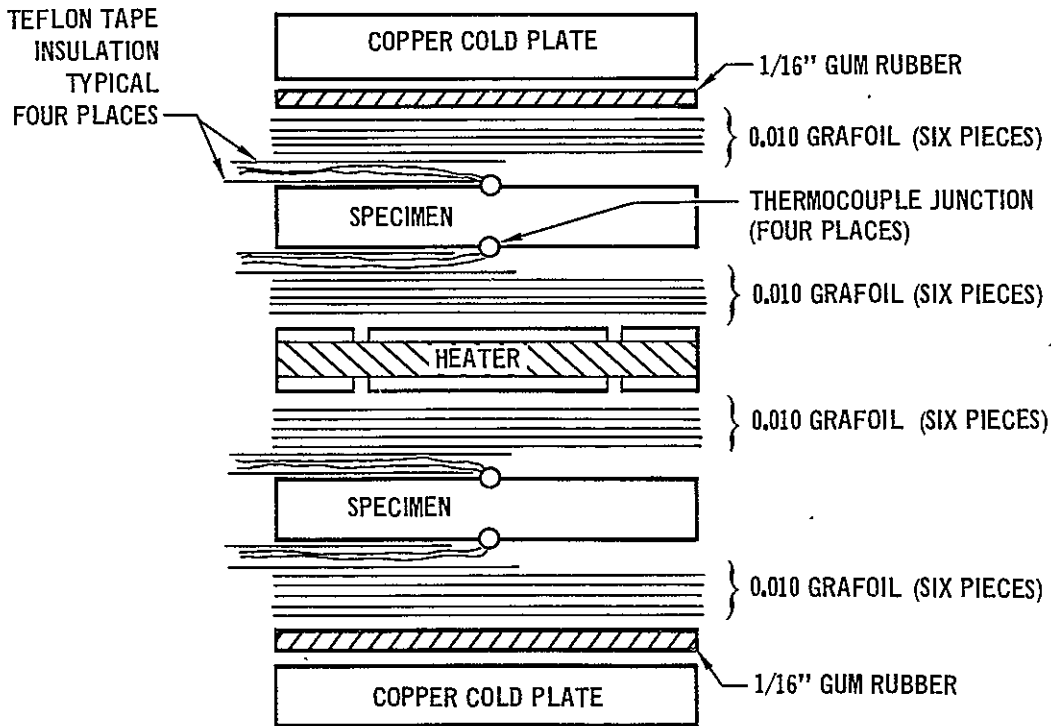


FIGURE 4. TEMPERATURE DROP ACROSS SPECIMEN IN VACUUM

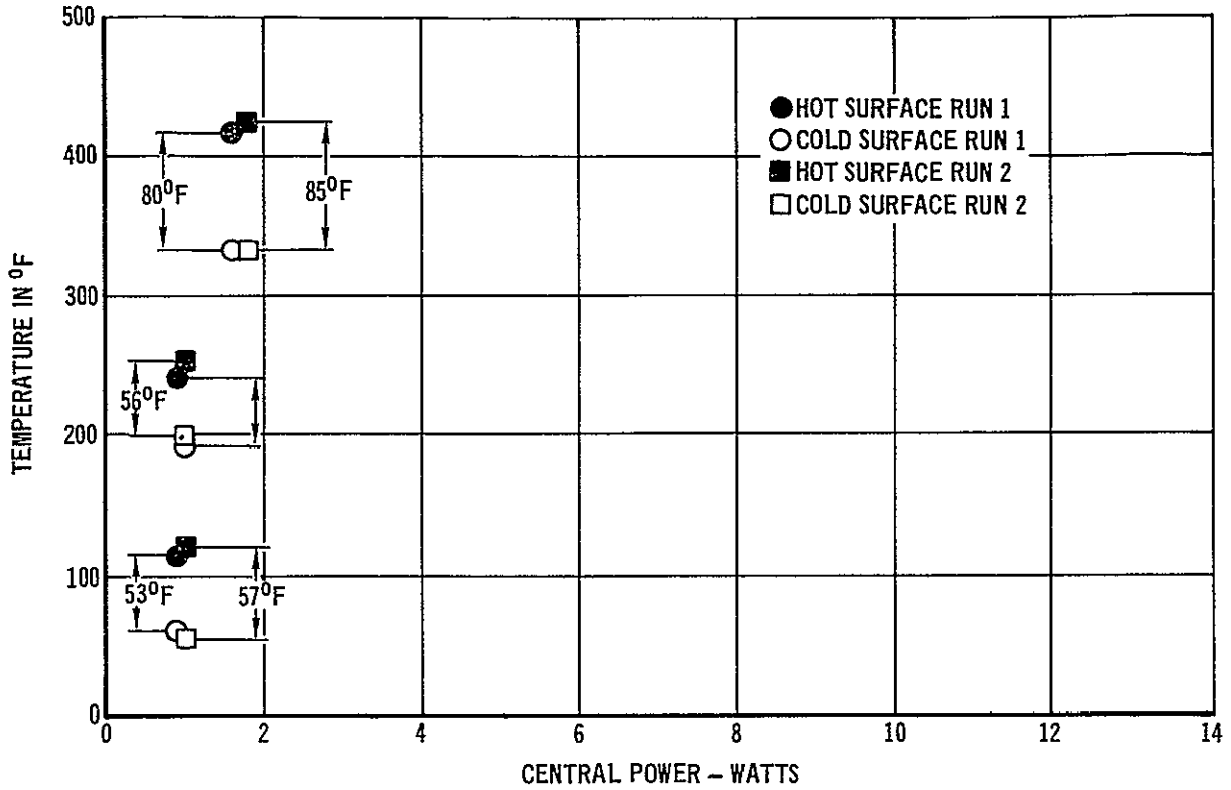


FIGURE 5 TEMPERATURE DROP ACROSS SPECIMEN IN NITROGEN GAS AT 1 ATMOSPHERE

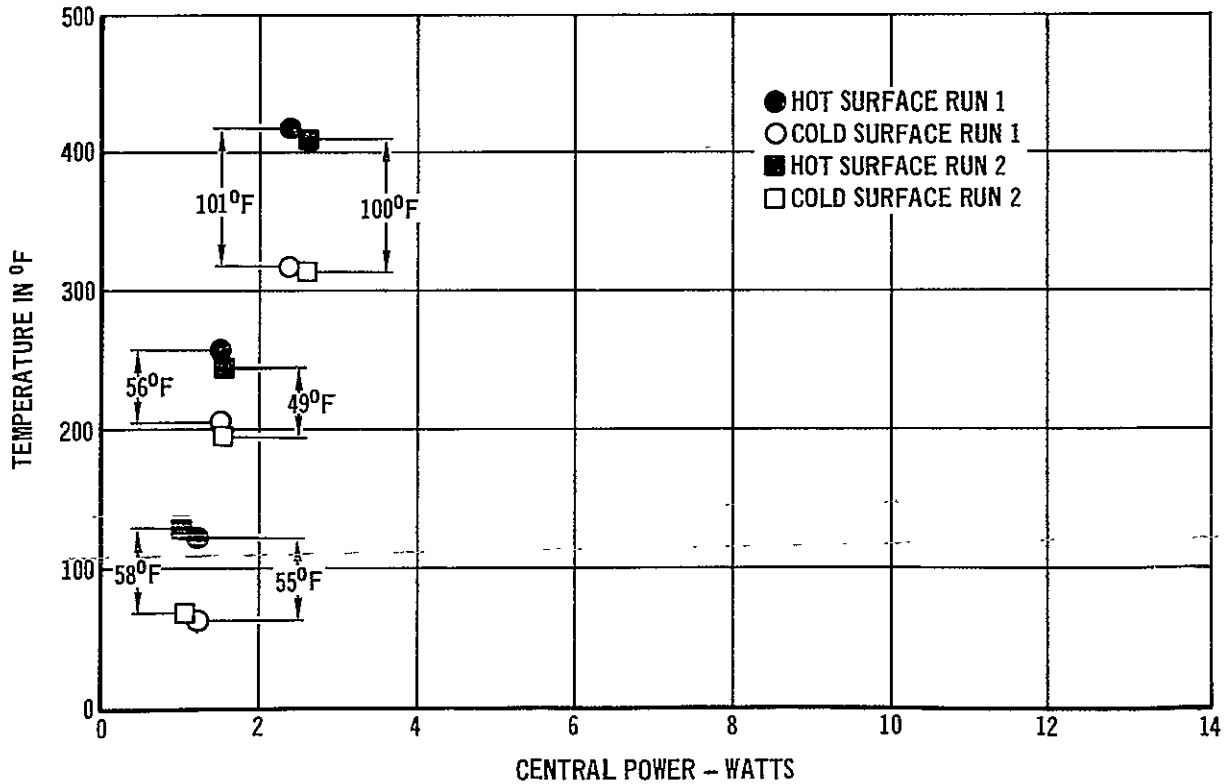


FIGURE 6 TEMPERATURE DROP ACROSS SPECIMEN IN HELIUM GAS AT 1 ATMOSPHERE

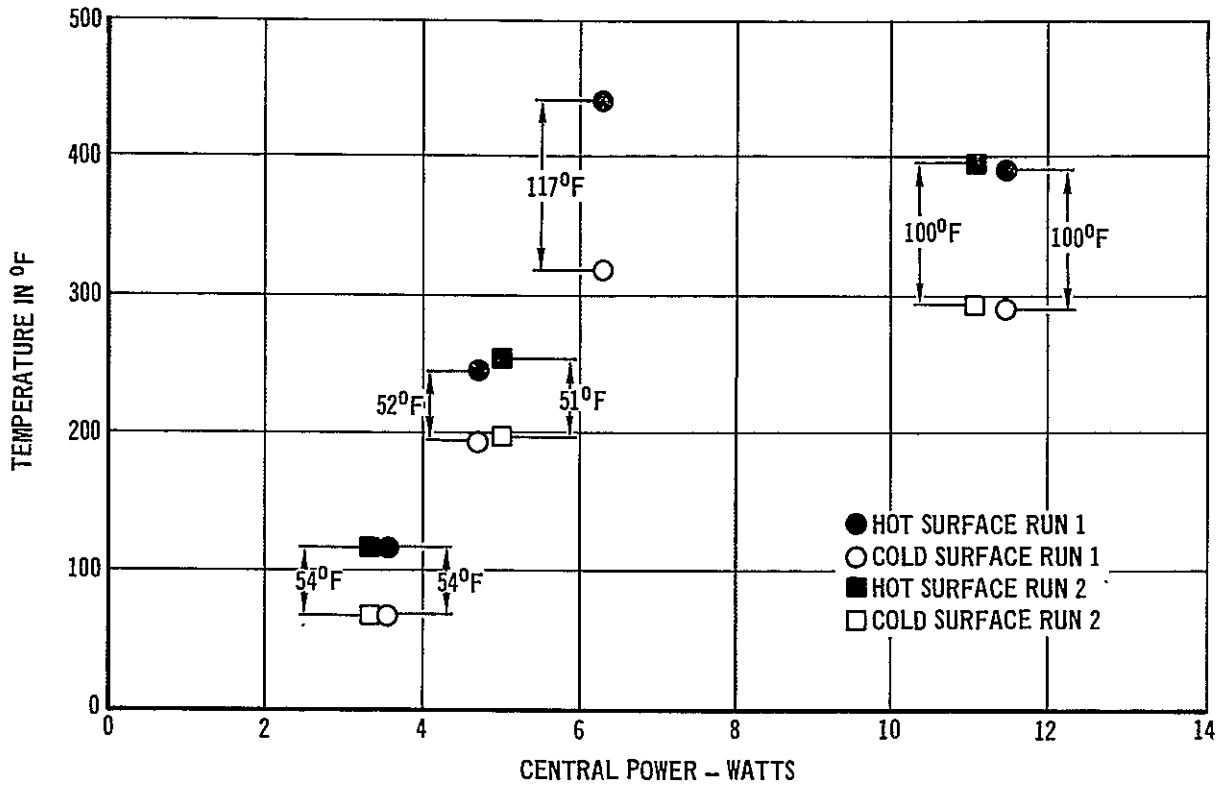


FIGURE 7 THERMAL CONDUCTIVITY OF POWDER FILLED HONEYCOMB SPECIMEN IN VACUUM

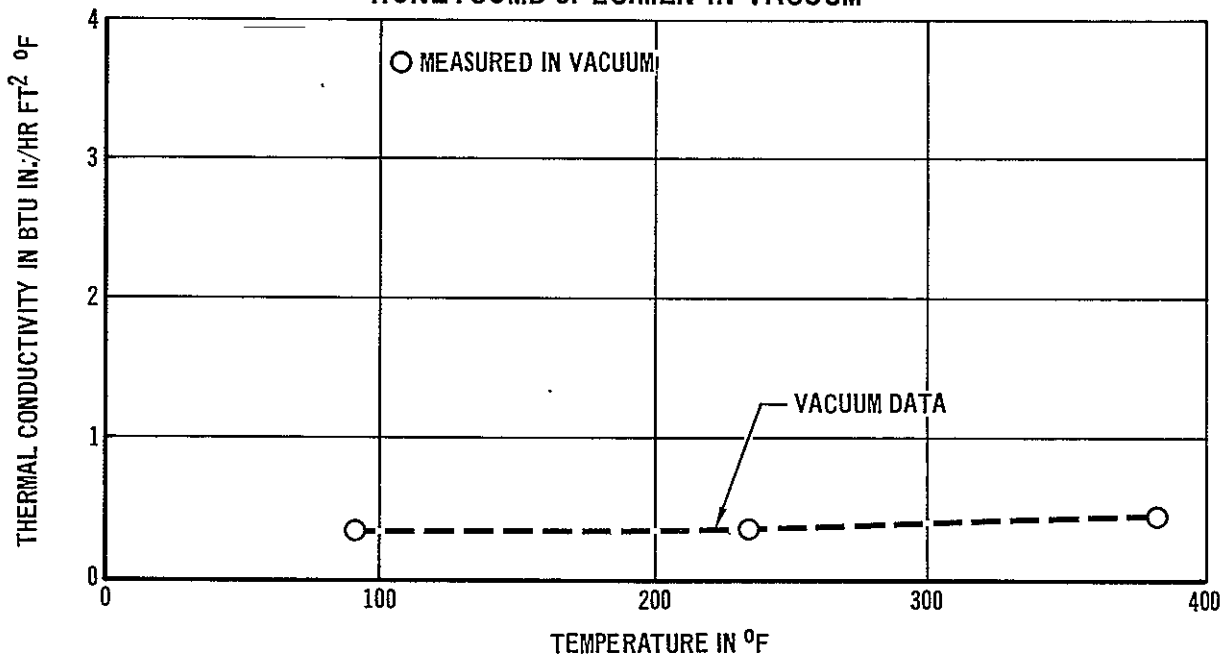


FIGURE 8 THERMAL CONDUCTIVITY OF POWDER FILLED HONEYCOMB SPECIMEN IN NITROGEN GAS AT 1 ATMOSPHERE

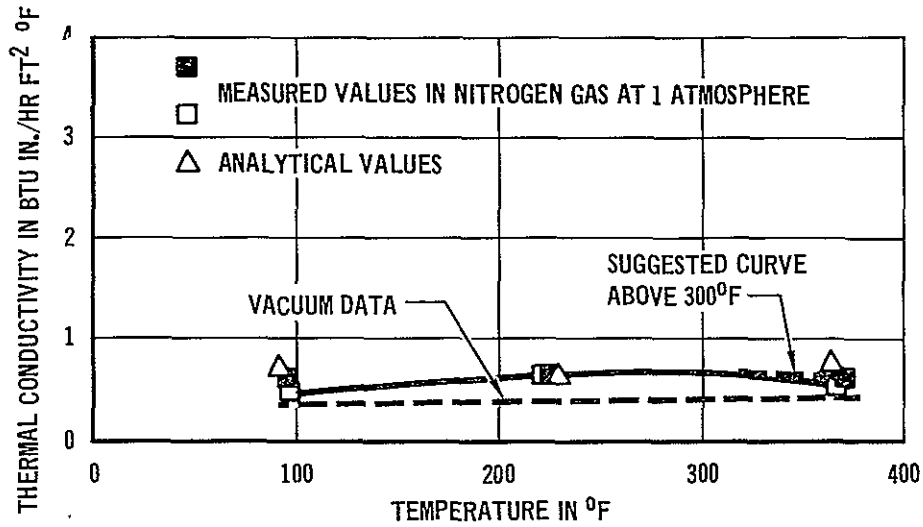


FIGURE 9 THERMAL CONDUCTIVITY OF POWDER FILLED HONEYCOMB SPECIMEN IN HELIUM GAS AT 1 ATMOSPHERE

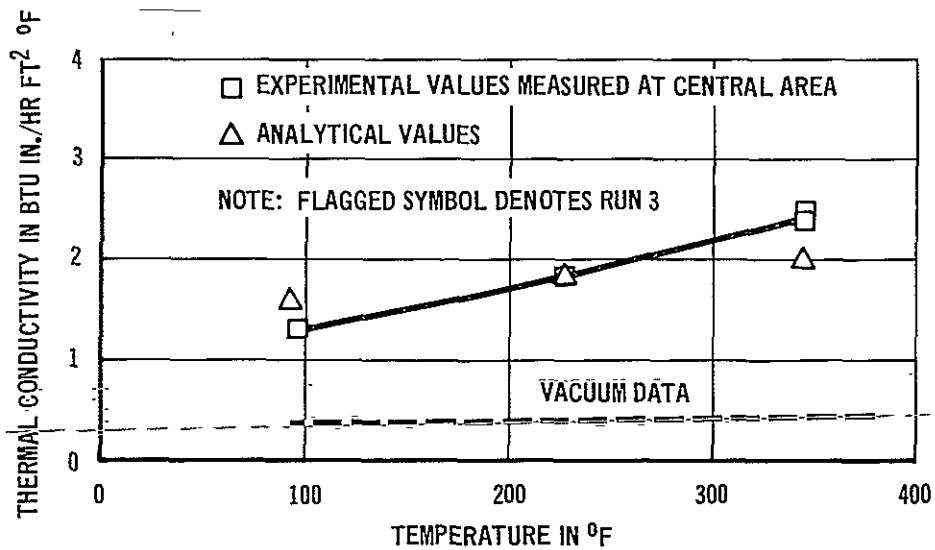


TABLE 1
COMPARISON OF ANALYTICAL AND EXPERIMENTAL VALUES

TEMP (°F)	THERMAL CONDUCTIVITY, $\frac{\text{BTU-IN.}}{\text{HR FT}^2 \text{ } ^\circ\text{F}}$	
	ANALYTICAL	EXPERIMENTAL
VACUUM		
93		0.361
228		0.381
378		0.439
NITROGEN GAS		
95	0.551	0.444
225	0.634	0.641
367	0.718	0.548
HELIUM GAS		
95	1.58	1.30
225	1.81	1.80
345	2.02	2.40

FIGURE 10 THERMAL CONDUCTIVITY OF POWDER FILLED HONEYCOMB-SPECIMEN IN VACUUM, HELIUM GAS, AND NITROGEN GAS AT 1 ATMOSPHERE

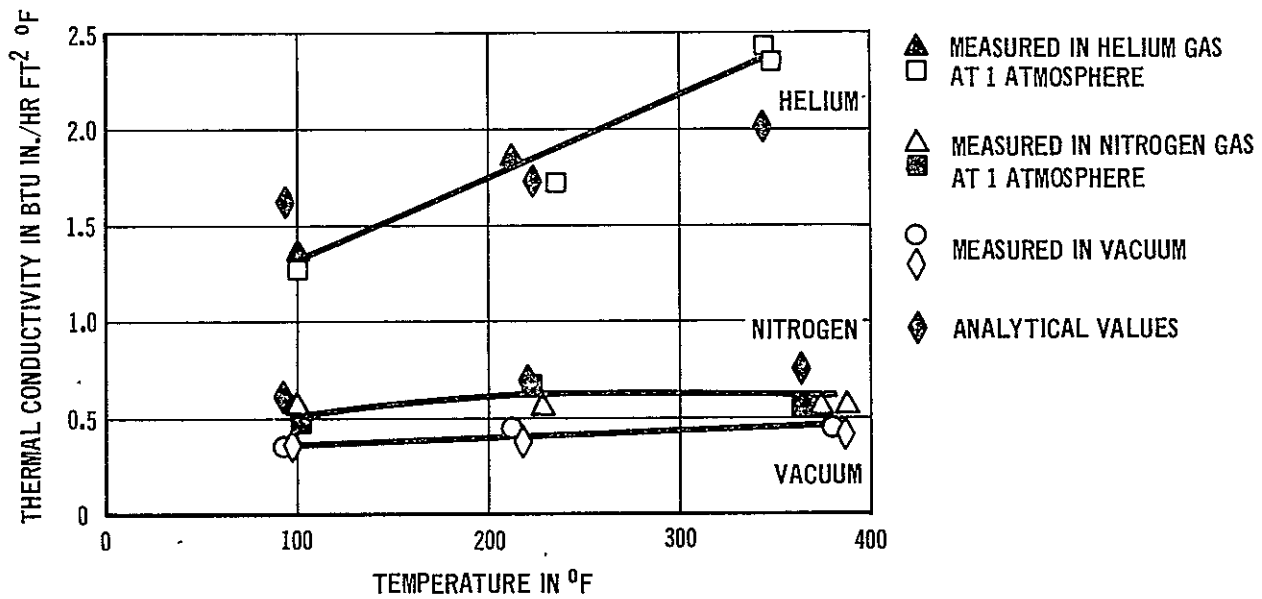


TABLE 2
THERMAL CONDUCTIVITY OF POWDER FILLED FIBERGLASS HONEYCOMB STRUCTURE
IN VACUUM ($\sim 2 \times 10^{-5}$ TORR) ENVIRONMENT
Measured in ASTM C177 Guarded Hot Plate Apparatus

RUN NO. 1 DATE AND TIME	AVERAGE SPECIMEN MEAN TEMP - °F	TOTAL HEAT INPUT WATTS	AVERAGE SPECIMEN ΔT °F	SPECIMEN GAGE IN.	SPECIMEN THERMAL CONDUCTIVITY BTU IN./HR FT ² °F
3:15 P.M. 9/30/75	92	0.89	52.80	1.077	0.356
3:50 P.M. 9/30/75	92	0.89	52.82	1.077	0.357
2:00 P.M. 10/7/75	216	0.99	47.52	1.077	0.439
2:30 P.M. 10/7/75	216	0.99	47.52	1.077	0.439
1:35 P.M. 10/7/75	375	1.69	79.69	1.077	0.446
2:10 P.M. 10/7/75	375	1.69	79.93	1.077	0.444

TABLE 3
THERMAL CONDUCTIVITY OF POWDER FILLED FIBERGLASS HONEYCOMB
STRUCTURE IN VACUUM ($\sim 1 \times 10^{-5}$ TORR) ENVIRONMENT
Measured in ASTM C177 Guarded Hot Plate Apparatus

RUN NO. 2 DATE AND TIME	AVERAGE SPECIMEN MEAN TEMP - °F	TOTAL HEAT INPUT WATTS	AVERAGE SPECIMEN ΔT °F	SPECIMEN GAGE IN.	SPECIMEN THERMAL CONDUCTIVITY BTU IN./HR FT ² °F
2:45 P.M. 10/24/75	93	0.98	56.73	1.075	0.361
3:45 P.M. 10/24/75	93	0.98	56.75	1.075	0.361
11:00 A.M. 10/29/75	228	1.01	55.72	1.075	0.381
11:35 A.M. 10/29/75	228	1.01	55.67	1.075	0.382
3:30 P.M. 10/31/75	378	1.78	85.09	1.075	0.439
4:00 P.M. 10/31/75	378	1.78	85.08	1.075	0.439

**TABLE 4 THERMAL CONDUCTIVITY OF POWDER FILLED FIBERGLASS HONEYCOMB
STRUCTURE IN NITROGEN ENVIRONMENT AT 1 ATM PRESSURE**

Measured in ASTM C177 Guarded Hot Plate Apparatus

RUN NO. 1 DATE AND TIME	AVERAGE SPECIMEN MEAN TEMP - °F	TOTAL HEAT INPUT WATTS	AVERAGE SPECIMEN ΔT °F	SPECIMEN GAGE IN.	SPECIMEN THERMAL CONDUCTIVITY BTU IN./HR FT ² °F
2:00 P.M. 9/29/75	96	1.33	55.11	1.077	0.510
2:30 P.M. 9/29/75	96	1.33	55.09	1.077	0.510
5:55 P.M. 10/3/75	228	1.52	55.78	1.077	0.574
6:25 P.M. 10/3/75	228	1.52	55.78	1.077	0.574
2:50 P.M. 10/14/75	370	2.46	100.48	1.077	0.517
4:25 P.M. 10/14/75	370	2.46	101.51	1.077	0.517
1:30 P.M. 10/16/75	382	2.93	111.23	1.077	0.554
2:00 P.M. 10/16/75	382	2.93	111.21	1.077	0.554

**TABLE 5 THERMAL CONDUCTIVITY OF POWDER FILLED FIBERGLASS HONEYCOMB
STRUCTURE IN NITROGEN ENVIRONMENT AT 1 ATM PRESSURE**

Measured in ASTM C177 Guarded Hot Plate Apparatus

RUN NO. 1 DATE AND TIME	AVERAGE SPECIMEN MEAN TEMP - °F	TOTAL HEAT INPUT WATTS	AVERAGE SPECIMEN ΔT °F	SPECIMEN GAGE IN.	SPECIMEN THERMAL CONDUCTIVITY BTU IN./HR FT ² °F
8:30 A.M. 10/25/75	98	1.25	58.16	1.075	0.444
9:30 A.M. 10/25/75	98	1.25	57.35	1.075	0.459
2:30 P.M. 10/25/75	222	1.50	49.20	1.075	0.641
3:05 P.M. 10/25/75	222	1.50	49.20	1.075	0.641
1:30 P.M. 10/31/75	367	2.60	99.77	1.075	0.548
2:00 P.M. 10/31/75	367	2.60	99.79	1.075	0.548

**TABLE 6 THERMAL CONDUCTIVITY OF POWDER FILLED FIBERGLASS HONEYCOMB
STRUCTURE IN HELIUM ENVIRONMENT AT 1 ATM PRESSURE**

Measured in ASTM C177 Guarded Hot Plate Apparatus

RUN NO. 1 DATE AND TIME	AVERAGE SPECIMEN MEAN TEMP - °F	TOTAL HEAT INPUT WATTS	AVERAGE SPECIMEN ΔT °F	SPECIMEN GAGE IN.	SPECIMEN THERMAL CONDUCTIVITY BTU IN./HR FT ² °F
2:50 P.M. 10/1/75	95	3.45	53.50	1.077	1.358
3:25 P.M. 10/1/75	95	3.45	53.54	1.077	1.357
4:40 P.M. 10/7/75	217	4.72	53.22	1.077	1.867
5:15 P.M.	217	4.72	53.22	1.077	1.867

**TABLE 7 THERMAL CONDUCTIVITY OF POWDER FILLED FIBERGLASS HONEYCOMB
STRUCTURE IN HELIUM ENVIRONMENT AT 1 ATM PRESSURE**

Measured in ASTM C177 Guarded Hot Plate Apparatus

RUN NO. 2 DATE AND TIME	AVERAGE SPECIMEN MEAN TEMP - °F	TOTAL HEAT INPUT WATTS	AVERAGE SPECIMEN ΔT °F	SPECIMEN GAGE IN.	SPECIMEN THERMAL CONDUCTIVITY BTU IN./HR FT ² °F
3:05 P.M. 10/27/75	95	3.33	54.85	1.075	1.279
3:45 P.M. 10/27/75	95	3.33	54.85	1.075	1.279
1:45 P.M. 10/29/75	226	4.87	56.87	1.075	1.800
2:15 P.M. 10/29/75	226	4.87	56.91	1.075	1.799
2:30 P.M. 11/3/75	344	11.163	99.07	1.075	2.370
3:00 P.M. 11/3/75	344	11.163	99.03	1.075	2.370
RUN NO. 3					
12:55 A.M. 11/10/75	342	11.47	100.12	1.075	2.408
1:30 P.M. 11/10/75	342	11.47	100.13	1.075	2.408